2M14

NATIONAL AERONAUTICS AND SPACE ADMINISTRATION

Technical Memorandum 33-679

Autonomous Manipulation on a Robot: Summary of Manipulator Software Functions

R. A. Lewis

(NASA-CR-137354) AUTONOMOUS MANIPULATION ON A ROBOT: SUMMARY OF MANIPULATOR SOFTWARE FUNCTIONS (Jet Propulsion Lab.) ~~86~~ 89 p HC $7.50 CSCL 14B

N74-20023

Unclas

G3/14 34350

JET PROPULSION LABORATORY

CALIFORNIA INSTITUTE OF TECHNOLOGY

PASADENA, CALIFORNIA

March 15, 1974

TECHNICAL REPORT STANDARD TITLE PAGE

1. Report No. T.M. 33-679	2. Government Accession No.	3. Recipient's Catalog No.
4. Title and Subtitle Autonomous Manipulation on a Robot: Summary of Manipulator Software Functions		5. Report Date March 15, 1974 6. Performing Organization Code
7. Author(s) Richard A. Lewis		8. Performing Organization Report No.
9. Performing Organization Name and Address JET PROPULSION LABORATORY California Institute of Technology 4800 Oak Grove Drive Pasadena, California 91103		10. Work Unit No. 11. Contract or Grant No. NAS 7-100 13. Type of Report and Period Covered
12. Sponsoring Agency Name and Address NATIONAL AERONAUTICS AND SPACE ADMINISTRATION Washington, D.C. 20546		14. Sponsoring Agency Code
15. Supplementary Notes		

16. Abstract

A six degree-of-freedom computer-controlled manipulator is examined, and the relationships between the arm's joint variables and 3-space are derived. Arm trajectories using sequences of third-degree polynomials to describe the time history of each joint variable are presented and two approaches to the avoidance of obstacles are given. The equations of motion for the arm are derived and then decomposed into time-dependent factors and time-independent coefficients. Several new and simplifying relationships among the coefficients are proven. Two sample trajectories are analyzed in detail for purposes of determining the most important contributions to total force in order that relatively simple approximations to the equations of motion can be used.

17. Key Words (Selected by Author(s))	18. Distribution Statement
Control and Guidance Robotics Artificial Intelligence	Unclassified - Unlimited

19. Security Classif. (of this report)	20. Security Classif. (of this page)	21. No. of Pages	22. Price
Unclassified	Unclassified	79	

NATIONAL AERONAUTICS AND SPACE ADMINISTRATION

Technical Memorandum 33-679

Autonomous Manipulation on a Robot: Summary of Manipulator Software Functions

R. A. Lewis

JET PROPULSION LABORATORY
CALIFORNIA INSTITUTE OF TECHNOLOGY
PASADENA, CALIFORNIA

March 15, 1974

Prepared Under Contract No. NAS 7-100
National Aeronautics and Space Administration

PREFACE

The work described in this report was performed by the Guidance and Control Division of the Jet Propulsion Laboratory.

PRECEDING PAGE BLANK NOT FILMED

ACKNOWLEDGEMENT

Special thanks are given to the Stanford Artificial Intelligence Project, particularly Dr. R. C. Paul, and V. D. Scheinman, without whose efforts we would have had little substantial foundation on which to build.

CONTENTS

CONTENTS (contd)

TABLES

FIGURES

ABSTRACT

A six degree-of-freedom computer-controlled manipulator is examined, and the relationships between the arm's joint variables and 3-space are derived. Arm trajectories using sequences of third-degree polynomials to describe the time history of each joint variable are presented and two approaches to the avoidance of obstacles are given. The equations of motion for the arm are derived and then decomposed into time-dependent factors and time-independent coefficients. Several new and simplifying relationships among the coefficients are proven. Two sample trajectories are analyzed in detail for purposes of determining the most important contributions to total force in order that relatively simple approximations to the equations of motion can be used.

I. INTRODUCTION

The Jet Propulsion Laboratory is engaged in a robot research program ("Artificial Intelligence for Integrated Robot Systems") aimed at the development and demonstration of the ability to integrate a variety of robotic functions. These functions include locomotion, manipulation, sensation, perception, and decision making. The immediate objective of the program is the building of a robot breadboard which demonstrates the integration of these capabilities and performs autonomous goal-directed coordination of the separate functions. Broad goals are provided by man.

The robot breadboard software is in two computers, a local minicomputer and a remote larger computer. The minicomputer is generally used as a real-time controller (RTC), being sequentially dedicated to the control of one of the functional subsystems (vehicle, manipulator, etc). The RTC is in direct communication with the breadboard hardware. The larger remote computer, generally considered as a timeshared computer (TSC) not dedicated to any one task, is used primarily for planning purposes. This report considers the functions performed by the manipulator software residing in the TSC. Manipulator kinematics, trajectory generation, obstacle avoidance, dynamics, and TSC software are discussed. The manipulator under consideration is a JPL-built modification of the Stanford Electric Arm (Refs. 1, 2), a six degree-of-freedom arm designed for computer control.

II. MANIPULATOR KINEMATICS

Manipulator kinematics have been analyzed and presented elsewhere (Refs. 3-9) and are summarized here only for clarity. This section, then, briefly describes general manipulator coordinate system conventions, applies these to the JPL manipulator, and presents the relations between joint-variable space and arm position/orientation.

A. Coordinate System Conventions

Consider a system of n mechanical links (numbered 1 through n), each capable of linear or rotary motion relative to the adjacent links. For reference, define link 0 to be fixed to a base (in a rigid table, on a vehicle, or on the ground, for instance). Define a joint to be the intersection of two adjacent links; in particular, joint i is the intersection of links i-1 and i, $i = 1, \ldots, n$.

Then (see Figs. 1, 2) define the following:

$\vec{z}_i \equiv$ axis of joint i+1 (sense arbitrary). If the joint is rotary, then $\vec{z}_i$ is the axis of rotation; if prismatic (i.e., linear), then $\vec{z}_i$ is in the direction of linear motion. Defining $\vec{z}_n$ in an arbitrary manner, $\vec{z}_i$ is defined for $i = 0, \ldots, n$.

$\vec{x}_i \equiv \vec{z}_{i-1} \times \vec{z}_i / \| \vec{z}_{i-1} \times \vec{z}_i \|$, the common normal between $\vec{z}_{i-1}$ and $\vec{z}_i$, directed from the former to the latter. If $\vec{z}_{i-1} \times \vec{z}_i = 0$, then $\vec{x}_i$ is arbitrary subject only to $\vec{x}_i \cdot \vec{z}_i = 0$. Defining $\vec{x}_0$ in an arbitrary manner (with $\vec{x_0} \cdot \vec{z_0} = 0$), $\vec{x}_i$ is defined for $i = 0, \ldots, n$.

$\vec{y}_i \equiv \vec{z}_i \times \vec{x}_i$, $i = 0, \ldots, n$.

Thus an orthonormal coordinate system $(\vec{x}_i, \vec{y}_i, \vec{z}_i)$, fixed in link i, $i = 0, \ldots n$, is defined. The following parameters define the relationship between successive coordinate systems:

$\theta_i \equiv$ angle from $\vec{x}_{i-1}$ to $\vec{x}_i$, measured positively counterclockwise about $\vec{z}_{i-1}$

$r_i \equiv$ distance along $\vec{z}_{i-1}$ from $\vec{x}_{i-1}$ to $\vec{x}_i$.

$\alpha_i \equiv$ angle from $\vec{z}_{i-1}$ to $\vec{z}_i$, measured positively counterclockwise about $\vec{x}_i$.

$a_i \equiv$ distance along $\vec{x}_i$ from $\vec{z}_{i-1}$ to $\vec{z}_i$.

A vector $\vec{v}_i$ expressed in system i can be expressed in system i-1 as $\vec{v}_{i-1}$ using the transformation T^i_{i-1}, as follows:

$$\vec{v}_{i-1} = T^i_{i-1}\ \vec{v}_i$$

More specifically, $\vec{v}_i$ is first rotated about $\vec{x}_i$ by $-\alpha_i$ (aligning $\vec{z}_i$ and $\vec{z}_{i-1}$), then translated along $\vec{x}_i$ by a_i (bringing $\vec{z}_i$ and $\vec{z}_{i-1}$ into coincidence), then translated along $\vec{z}_i$ ($\equiv\vec{z}_{i-1}$) by r_i (giving $\vec{x}_i$ and $\vec{x}_{i-1}$ a common origin), and finally rotated about $\vec{z}_i$ by $-\theta_i$ (bringing the two systems into coincidence).

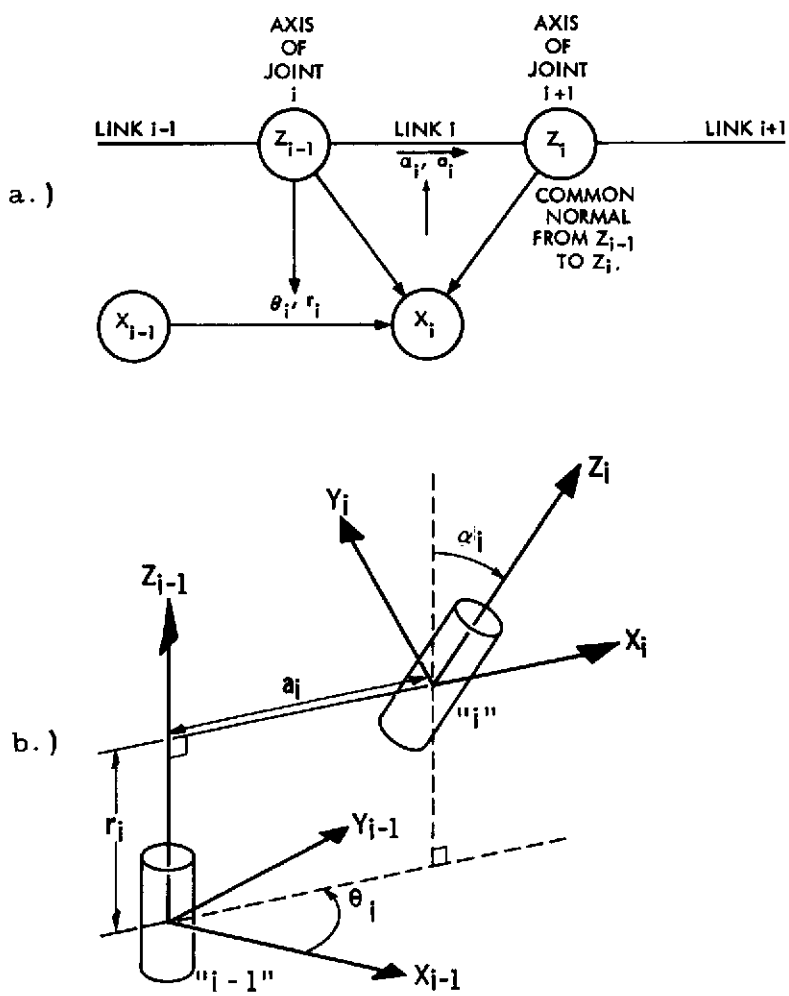

Fig. 1. Standard Manipulator Parameters

Thus,

$$T^{i}_{i-1} = \begin{bmatrix} c_{\theta_i} & -s_{\theta_i} & 0 & 0 \\ s_{\theta_i} & c_{\theta_i} & 0 & 0 \\ 0 & 0 & 1 & 0 \\ 0 & 0 & 0 & 1 \end{bmatrix} \begin{bmatrix} 1 & 0 & 0 & 0 \\ 0 & 1 & 0 & 0 \\ 0 & 0 & 1 & r_i \\ 0 & 0 & 0 & 1 \end{bmatrix} \begin{bmatrix} 1 & 0 & 0 & a_i \\ 0 & 1 & 0 & 0 \\ 0 & 0 & 1 & 0 \\ 0 & 0 & 0 & 1 \end{bmatrix} \begin{bmatrix} 1 & 0 & 0 & 0 \\ 0 & c_{\alpha_i} & -s_{\alpha_i} & 0 \\ 0 & s_{\alpha_i} & c_{\alpha_i} & 0 \\ 0 & 0 & 0 & 1 \end{bmatrix}$$

$$T^{i}_{i-1} = \begin{bmatrix} c_{\theta_i} & -c_{\alpha_i} s_{\theta_i} & s_{\alpha_i} s_{\theta_i} & a_i c_{\theta_i} \\ s_{\theta_i} & c_{\alpha_i} c_{\theta_i} & -s_{\alpha_i} c_{\theta_i} & a_i s_{\theta_i} \\ 0 & s_{\alpha_i} & c_{\alpha_i} & r_i \\ 0 & 0 & 0 & 1 \end{bmatrix} \qquad (1)$$

where $s_x \equiv \sin(x)$ and $c_x \equiv \cos(x)$.

Since the axes of motion are $\vec{z}_i$ (by definition), then a_i and α_i are constant for all i; either θ_i (if the joint is linear) or r_i (if rotary) is constant for each i.

The upper left 3×3 partition of T^{i}_{i-1} expresses the rotation of frame i relative to frame i-1. The upper right 3×1 partition expresses the position of the origin of frame i relative to i-1.

B. The JPL Manipulator

The JPL arm (Fig. 2) is characterized by the constant parameters a_i, α_i, r_i $(i \neq 3)$ and θ_3 given in Table 1. All joints except the third are rotary. The joint variables θ_i $(i \neq 3)$ and r_3 form the joint-variable vector $\vec{\theta}$ given by

$$\vec{\theta} \equiv (\theta_1, \theta_2, r_3, \theta_4, \theta_5, \theta_6).$$

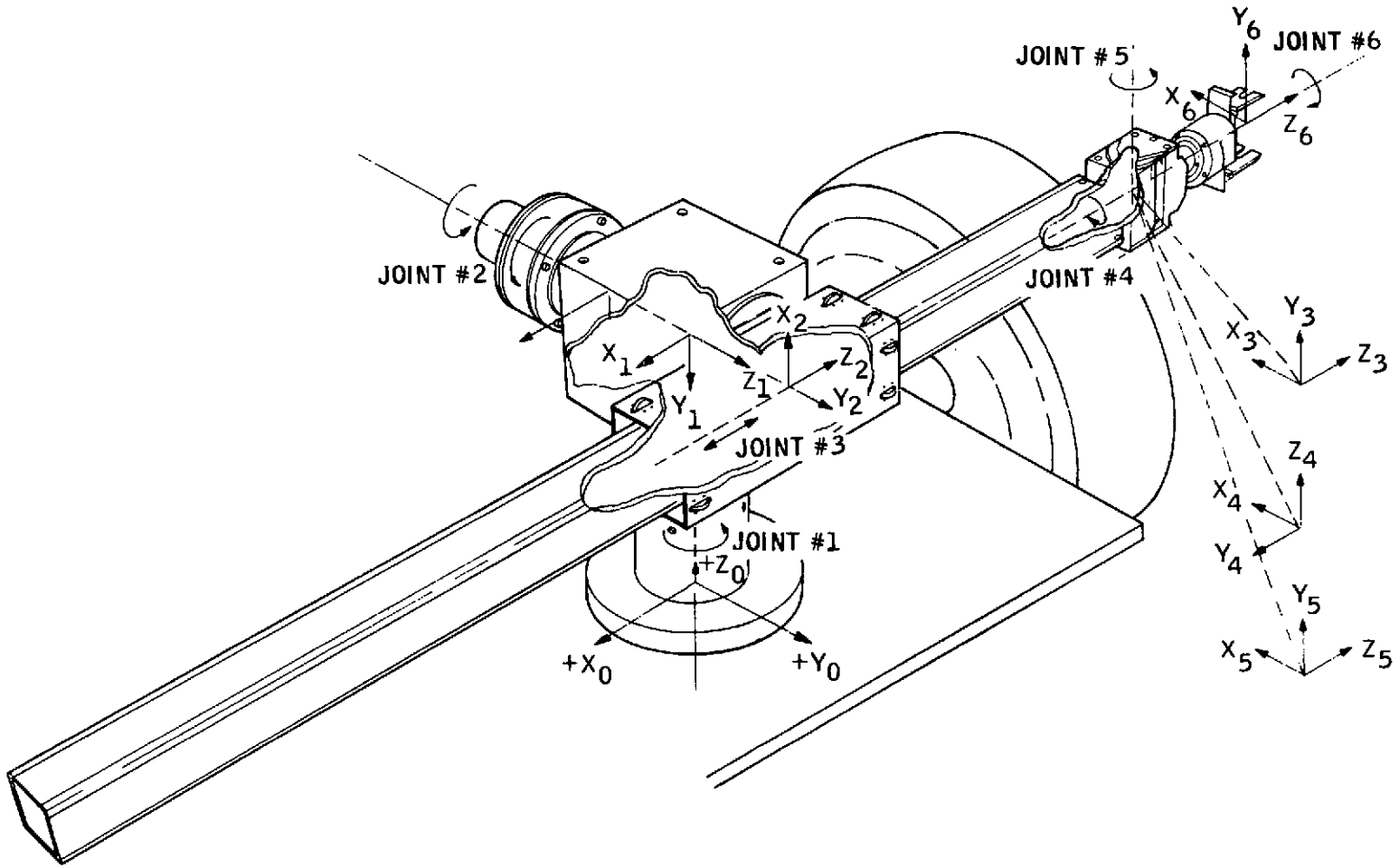

Figure 2. Reference Frames for Link-Joint Pairs of Arm

Table 1. The JPL Manipulator

i	α_i (deg)	r_i (cm)	θ_i (deg)	a_i (cm)	Maximum radial dimension about z_i (cm)	Maximum linear extension along $-z_i$ (cm)
1	-90	35.56	[-175, 175]	0	6.67	0
2	90	16.19	[-175, 175]	0	6.99	30.48
3	0	[14.0, 111.8]	-90	0	3.18	139.70 - r_3
4	-90	0	[-175, 175]	0	6.03	0
5	90	0	[-110, 110]	0		0
6	0	24.77	[-175, 175]	0		0
fingers	12.7 cm long, 3.02 cm wide, open to 5.72 cm each					

Note: The ranges of the six joint variables are indicated in brackets above.

The vectors $\vec{x}_0$ and the $\vec{z}_i$ i = 0, ..., 6, are defined as in Fig. 2. It is convenient to define four additional vectors (Fig. 3):

the approach vector $\vec{a} \equiv \vec{z}_6$, pointing in the direction of approach of the hand;

the sliding vector $\vec{s} \equiv \vec{y}_6$, pointing in the direction of finger motion as the hand opens and closes;

the normal vector $\vec{n} \equiv \vec{x}_6$, orthogonal to the plane of the fingers;

and the position vector $\vec{p}$, pointing from the origin of the base system to the origin of the hand system $(\vec{n}, \vec{s}, \vec{a})$.

Applying the arm parameters of Table 1 to the transformations T^i_{i-1} defined in Eq. (1) yields the six transformations T^i_{i-1}, i = 1, ...6, given in Appendix 1. The arm transformation T is given by

$$T \equiv T^6_0 = T^1_0 T^2_1 T^3_2 T^4_3 T^5_4 T^6_5.$$

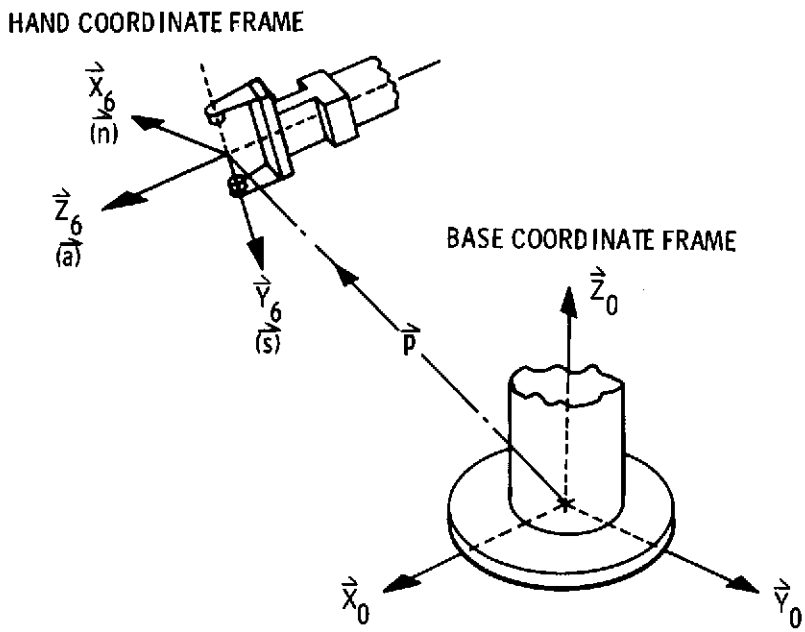

Fig. 3. Hand Position and Orientation Expressed in Base Coordinates

The columns of T are respectively, the normal, sliding, approach, and position vectors defined above. T is expressed in full in Appendix 1.

The arm is mounted on the vehicle as in Fig. 4 such that $\vec{z}_o$ is directed upwards from the vehicle orthogonal to the plane of the vehicle platform and $\vec{y}_o$ points ahead in the direction the vehicle is aimed. $\vec{x}_o$ is to the right. *

The origin of this system is the point on the vehicle platform at the center of the post comprising link 1.

Note that $\vec{z}_o$ is not in general colinear with the gravity vector. The vehicle platform may not be gravitationally horizontal.

*Where otherwise unspecified, the terms "right" and "left" are used with respect to an observer standing on his feet facing in the direction of $\vec{y}_o$.

The physical construction of the arm and the potentiometers permits only 350 deg of rotation for joints 1, 2, 4, and 6 and 220 deg for joint 5. The 10 deg (140 deg for joint 5) of deadband can be placed anywhere and are specified below and in Table 1. The joint variable r_3 is constrained by hardware to motion within the limits given in Table 1.

The first joint variable, θ_1, varies from -175 deg to +175 deg. θ_1 is 0 deg when (the boom side of) the shoulder (i.e., the link 3 side of link 2) is pointed straight ahead (i.e., in the direction of $\vec{y}_0$). θ_1 = +90 deg or -90 deg puts the shoulder to the left or right, respectively. The shoulder cannot point closer than 5 deg to the rear of the vehicle.

Coordinate system 1 ($\vec{x}_1, \vec{y}_1, \vec{z}_1$) is located at the intersection of the centers of the post and shoulder. θ_2 varies also from -175 deg to +175 deg and is 0 deg when the hand side of the boom is directed straight up (i.e., along $\vec{z}_0$). When $\theta_2 > 0$ the arm looks like a human left arm; when $\theta_2 < 0$, the arm is a right arm. Where feasible, the arm will not "flip" (over the top) from right to left or left to right. There will, however, be occasions

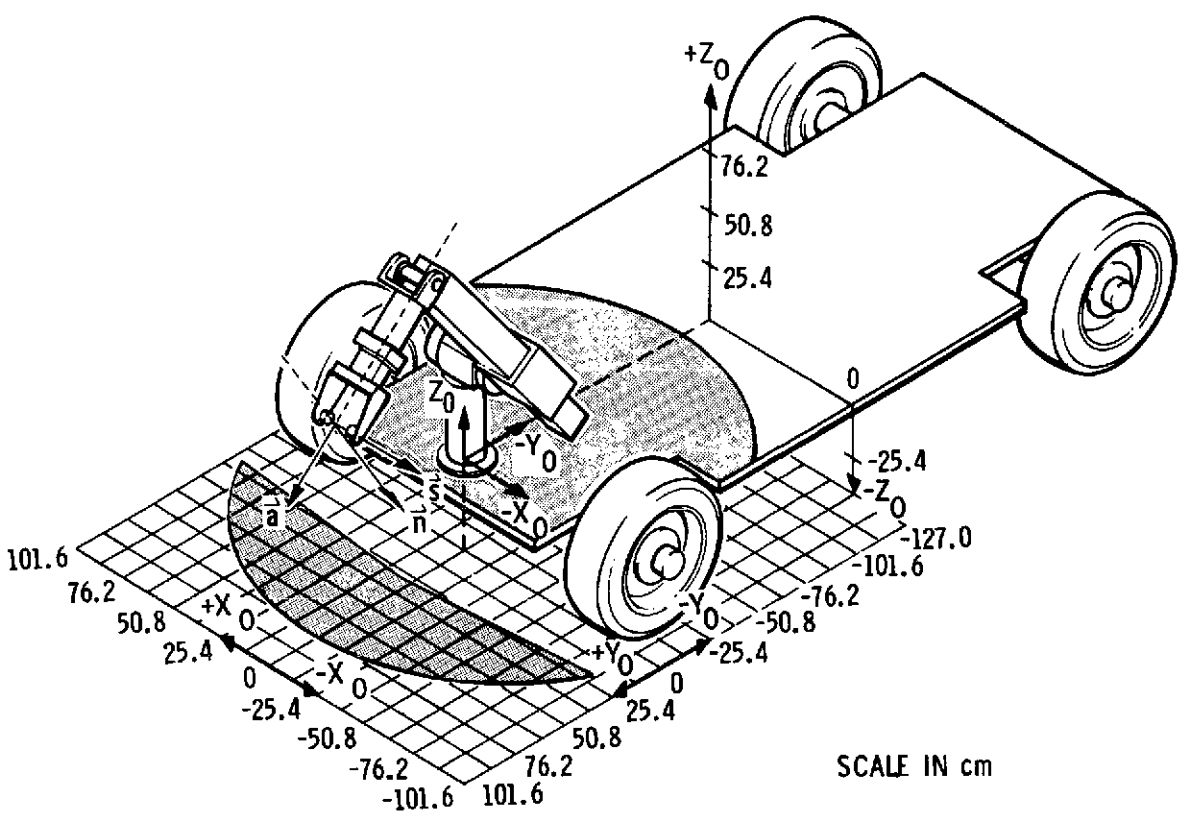

Fig. 4. Arm on Vehicle Base and Hand Coordinates

on which the flip motion is desirable if not mandatory. The deadband for θ_2 is straight down.

Coordinate system 2 $(\vec{x}_2, \vec{y}_2, \vec{z}_2)$ is located at the intersection of the centers of the shoulder and boom.

Coordinate systems 3, 4, and 5 are all located at the common intersection of $\vec{z}_3$, $\vec{z}_4$, and $\vec{z}_5$. θ_4 varies from -175 deg to +175 deg and, when θ_4 is 0 deg and θ_2 is -90 deg (as in Fig. 3), the axis $\vec{z}_4$ of joint 5 is up (along $\vec{z}_0$). The deadband of joint 4 is thus in the opposite direction. Joint 5 varies only from -110 deg to +110 deg in order that the hand not crash into the boom. θ_5 is 0 deg when the wrist is directed as an extension of the boom. The deadband is where the wrist is directed back up the boom.

θ_6 varies from -175 deg to +175 deg and, when 0 deg, the sliding axis is along the axis $\vec{z}_4$ of joint 5 (as in Fig. 3).

C. Kinematic Solutions

Given a joint-variable vector $\vec{\theta}$, the position/orientation of the terminal effector is described by

$$T = T(\vec{\theta}) \equiv T_0^6 = \begin{bmatrix} \vec{n} & \vec{s} & \vec{a} & \vec{p} \\ 0 & 0 & 0 & 1 \end{bmatrix}$$

There are four solutions to the problem of finding the joint-variable vector $\vec{\theta}$ yielding a given position/orientation T, two for a right-arm configuration ($\theta_2 < 0$) and two for a left-arm configuration ($\theta_2 > 0$). For each configuration there is one solution with θ_5 positive and another with θ_5 negative.

Briefly, the solutions are found by the following procedure. (For details see Appendix 2a.) Define a vector

$$\vec{d} = \begin{bmatrix} d_1 \\ d_2 \\ d_3 \end{bmatrix} = \vec{p} - r_6\vec{a} - \begin{bmatrix} 0 \\ 0 \\ r_1 \end{bmatrix},$$

the shoulder-to-end-of-boom vector. The boom extension length r_3 is found by noting that $\|d\|^2 = r_2^2 + r_3^2$. The joint 2 cosine is given by d_3/r_3, giving rise to the two possible values for θ_2. The value of θ_1 is computed from the first two components of $\vec{d}$ as

$$\theta_1 = \tan^{-1}\left[\frac{d_2 r_3 s_2 - d_1 r_2}{d_1 r_3 s_2 + d_2 r_2}\right]$$

Thus the first three joint variables are known, giving the base system-boom transformation T_0^3. Considering T_0^3 to be of the form

$$\begin{bmatrix} \vec{x}_3 & \vec{y}_3 & \vec{z}_3 & \vec{p}_3 \\ 0 & 0 & 0 & 1 \end{bmatrix}$$

and defining a reference vector $\vec{z}$ as the unit vector in the direction $\vec{z}_3 \times \vec{a}$, the remaining joint variables are found to be

$$\theta_4 = \tan^{-1}\left[\frac{\vec{y}_3 \times \vec{z} \cdot \vec{z}_3}{\vec{y}_3 \cdot \vec{z}}\right], \quad \theta_5 = \tan^{-1}\left[\frac{\vec{z}_3 \times \vec{a} \cdot \vec{z}}{\vec{z}_3 \cdot \vec{a}}\right], \text{ and}$$

$$\theta_6 = \tan^{-1}\left[\frac{\vec{z} \times \vec{s} \cdot \vec{a}}{\vec{z} \cdot \vec{s}}\right]$$

If $(\theta_4, \theta_5, \theta_6)$ are solution values, then so also are $(\theta_4 + \pi, -\theta_5, \theta_6 + \pi)$.

For very slight hand position/orientation changes the rates of change of joint variable with respect to position/orientation change may be computed. The details of arriving at the required incremental changes in the joint variables are described in Appendix 2b.

III. TRAJECTORIES AND OBSTACLES

In this section various constraints on moving the manipulator from one position/orientation to another are compared with the objectives of such motion to yield the currently implemented trajectory form. The term "trajectory" is here meant to refer to the partial or complete description of the path that the arm follows.

A. General Considerations

Four constraints are imposed on the form of the planned trajectory. First, continuity of joint variable (position) and its first two time derivatives (velocity, acceleration) must be guaranteed. Second, the trajectory must be readily calculable in a noniterative manner. Third, extraneous motion must be minimized. Finally, it must be possible (and straightforward) to determine and specify intermediate conditions (i. e. positions); collision detection and avoidance and possibly other functions cannot otherwise be served deterministically. (See below.)

The trajectory form may vary along a deterministic/conditional continuum, depending on the degree to which it is to respond to external sensory data during trajectory execution. At one extreme is a purely deterministic trajectory, planned completely in advance of execution. Only a catastrophe halts execution of the planned path. In this case, any external sensing to be done is performed during the planning stage. Internal sensing (of joint-variable state) is used throughout execution to maintain the adherence of actual motion to plan. Deterministic planning assumes a static world during arm motion as well as sufficient a priori knowledge and execution accuracy; adaptive control is limited.

Towards the other extreme is conditional planning, the nature of which is highly dependent on the specific external sensors used. Conditional planning brings response flexibility and possible planning time reduction at possible increased real-time computation requirement costs. It is currently intended that a conditional overlay to a deterministic trajectory plan be implemented. Since the nature, number, and placement of rapid response external sensors for the JPL robot is as yet unspecified in sufficient detail, only the deterministic trajectory is described below.

A related distinction concerns the manner in which the trajectory plan is specified. Either a sequence of two or more points can be selected ("point-to-point" trajectory), or the complete time history of the path ("path" trajectory) can be specified. In the obstacle-rich environment in which the JPL manipulator is to work, path planning must be selected in order to be able to effectively detect collisions in the plan.

Path planning can be conducted in either joint-variable space or in 3-space. In the former case, the time history of each joint is planned; it is the combination of the time histories of the joint variables that describe the motion of the arm. In the latter case, it is the motion of a particular point on the manipulator (commonly a point on the hand) that is planned; the required joint variable time histories are derived from the plan. Planning in joint variable space is implemented. The advantage of this selection is that the plan is formulated more directly in terms of the variables to be controlled during motion. The associated disadvantage is the difficulty in determining where the various links will be during motion, a task required to guarantee obstacle avoidance.

B. Polynomial Trajectories

In both the JPL Robot Research Program and the Stanford Hand-Eye Project (Ref. 6), the emphasis to date has been on deterministic path planning in joint variable space. Specifically, the time histories of the joint variables are specified as polynomial sequences. Continuity of joint variable position, velocity and acceleration can be guaranteed, intermediate positions can easily be specified and determined, the trajectories are readily calculable noniteratively, and it is possible to reduce extraneous motion to negligible amounts using polynomial trajectories.

If the trajectory for a given joint uses p polynomials, then $3(p + 1)$ coefficients are required to specify initial and terminal conditions (position, velocity, acceleration) and guarantee continuity of these variables at polynomial boundaries. An additional coefficient is required for each intermediate condition (position, for example) specified. Generally two intermediate positions are specified, one near departure and one near arrival, in order that safe departure and approach directions can be more directly controlled. Thus, one

seventh degree polynomial for each joint would suffice; so also would two cubics and a quintic (3, 5, 3), two quartics and a cubic (4, 3, 4), or five cubics. Only the last three sequences are considered here.

Fig. 5a shows the time history of a joint variable described by a cubic, a quintic, and another cubic. It has been found that trajectories using polynomials of degree five or higher typically wander, as shown. This behavior appears in observation as gross extraneous motion of the arm.

For single-segment trajectories (those for which no intermediate positions are specified), the quintic illustrated in Fig. 5b provides motion without wandering. This quintic has been presented in Ref. 6 and applies to incremental motion of joints. (This "incremental quintic" is used in conjunction with the incremental joint variable solutions of Appendix 2b).

Use of a quartic-cubic-quartic trajectory reveals a somewhat different problem. As shown in Fig. 5c, the desire to assure an appropriate direction of departure and approach of the terminal effector can be thwarted by the tendency of the quartic-cubic-quartic trajectory to overshoot or undershoot its endpoint values.

A third polynomial sequence, five cubics, is being implemented for the JPL arm. This trajectory appears to minimize the "wander" and "overshoot" problems. Typically, as in Fig. 5d, there is no overshoot; wander, when it occurs, is small.

The five cubic trajectory permits easy modification for obstacle avoidance, as does the (4, 3, 4) trajectory. In avoiding an obstacle quite often a single intermediate position for a joint will be added. This necessitates the addition of only a single cubic with its four coefficients; one coefficient is used to satisfy the new condition and the other three maintain continuity of θ, v, and a.

The determination of the relative times for the three main trajectory segments is accomplished initially by a heuristic. After modifying the trajectories, however, the desired maximum joint accelerations may be exceeded. By evaluating the accelerations for each trajectory segment for each joint at their extreme (the end points, since acceleration, the second derivative of a cubic, is linear), the maximum acceleration relative to the limit of

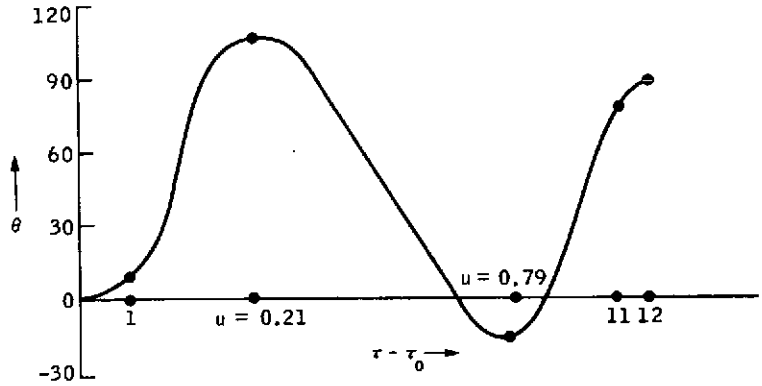

a) Sequence of Cubic-Quintic-Cubic Polynominal Segments (Showing "Wandering")

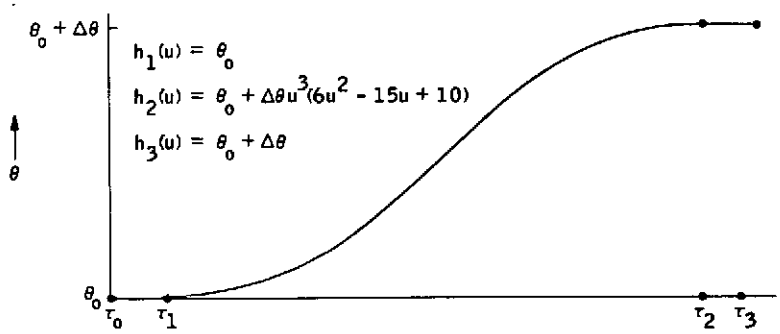

b) The "Incremental Quintic"

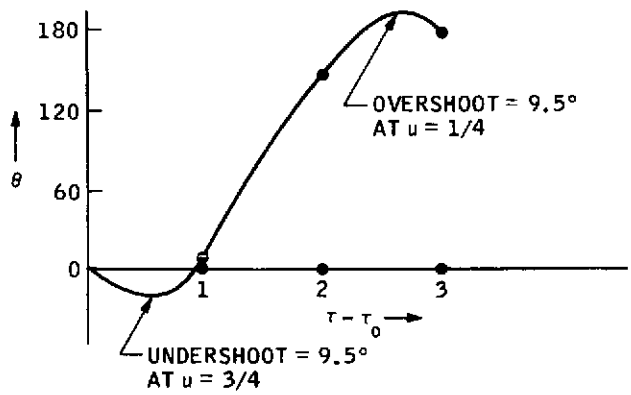

c) Sequence of Quartic-Cubic-Quartic Polynominal Segments (Showing "Overshoot")

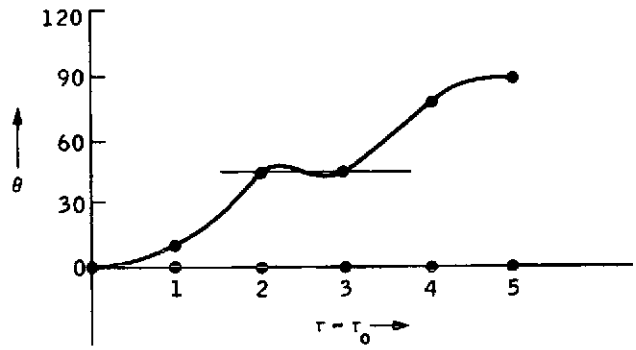

d) Sequence of Five Cubic Polynominal Segments

Figure 5. Various Polynominal Joint Trajectories

acceleration can be determined and then all time intervals t_i scaled up proportionate to the square root of the excess acceleration rates. This guarantees observation of the acceleration limits and also obviates the need to recompute polynomial coefficients. On all the polynomial trajectories considered above the coefficients remain constant under changes in the t_i if the ratios t_i/t_j remain constant for all i and j; multiplying all times by a constant leaves all polynomial coefficients unchanged.

C. Obstacle Classification, Detection, and Avoidance

In this section, the problems of classifying, detecting, and avoiding obstacles are discussed. Two methods of dealing with obstacles permanently fixed to the vehicle is presented, and alternative strategies for avoiding obstacles in the environment are also described.

1. Classification

The purpose of classifying obstacles is to form an exhaustive list of obstacles in order that all collisions can be considered in assuring the safety of planned arm motion. One possible taxonomic representation of disastrous occurrences to be avoided is presented here and summarized in Table 2.

The manipulator itself is an obstacle. The hand (link 6) is capable of colliding with the portion of the shoulder (link 2) extending away from the boom (link 3). The hand can also hit the support post (link 1) or the arm mounting base (see Fig. 6). Furthermore, each joint is limited in its motion. These joint stops are considered here as obstacles, for one way of avoiding commands that violate these stops is also a feasible way of dealing with other obstacles. Since these manipulator internal obstacles are always present, they are considered here as a type of permanent obstacle.

Vehicular obstacles, consisting of all vehicle mounted hardware capable of colliding with the arm (see Fig. 7), are also permanent. The TV/laser system, the vehicle platform surface and edges, the wheels, and the wheel drive motors comprise the set of permanent vehicle obstacles.

All of these but the platform itself move with respect to the manipulator base coordinate system ($\vec{x}_0$, $\vec{y}_0$, $\vec{z}_0$). The volumes occupied by the TV/laser, wheels, and motors can be based on either an assumed standard position, calculated using the actual steering angle and TV/laser pan and tilt,

Table 2. Obstacles and Colliders

OBSTACLES

1. Internal (permanent)
   - 1.1 Joint stops
   - 1.2 Link 1
     - 1.2.1 Support post
     - 1.2.2 Base
   - 1.3 Link 2 (shoulder)

2. Vehicular (permanent)
   - 2.1 TV/Laser (envelope, assumed position, or variable position) and support
   - 2.2 Wheels (assumed position, envelope, or variable position)
   - 2.3 Wheel motors (assumed position, envelope, or variable position)
   - 2.4 Platform
   - 2.5 Frame edge

3. Environmental (nonpermanent)
   - 3.1 Placed on vehicle
   - 3.2 In natural state

4. Two Arms (nonpermanent)

COLLIDERS

Link 3 (boom)
- Boom front (= hand rear)
- Boom rear
- Boom edge

Link 6 (hand)
- Hand front
- Hand side

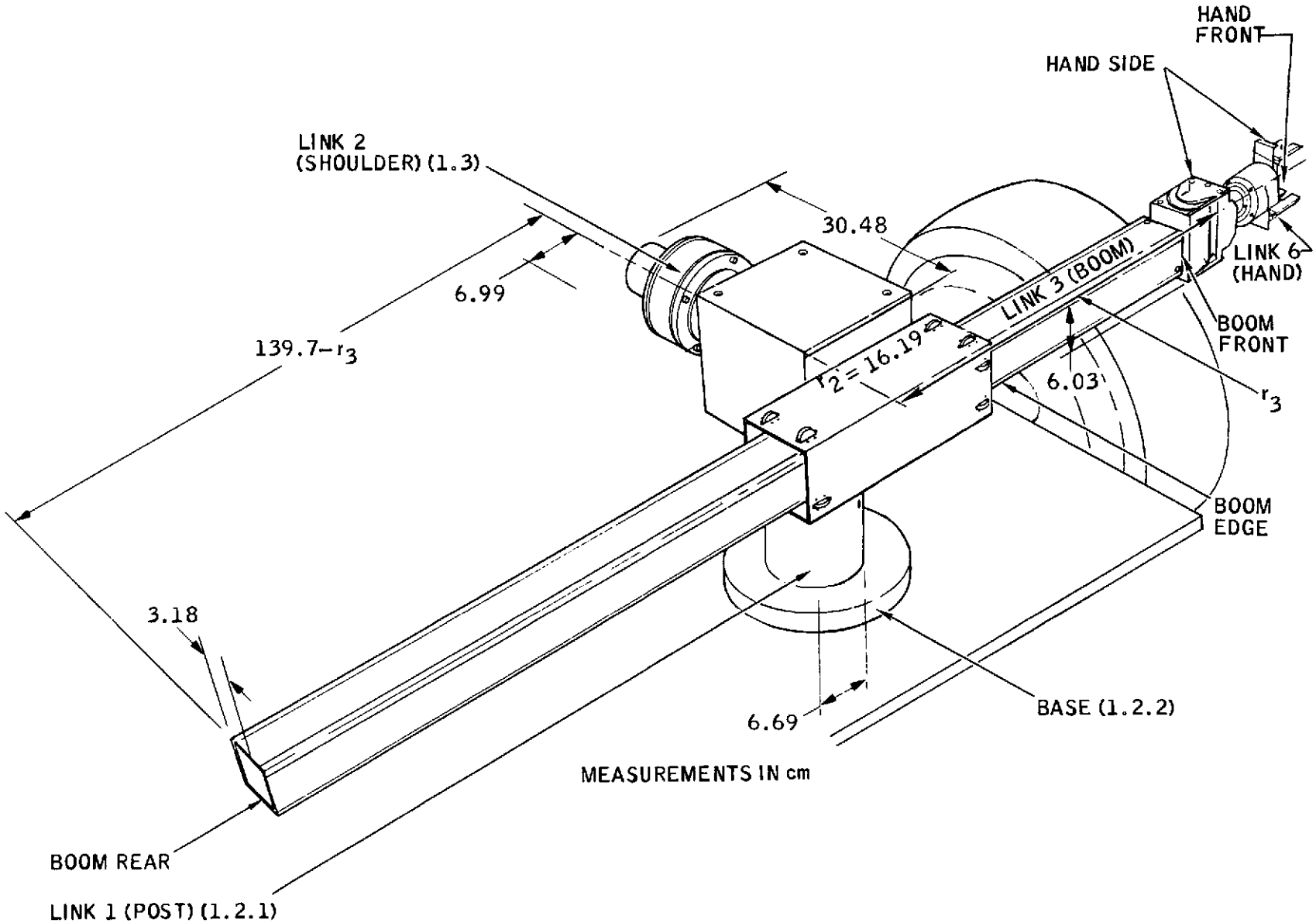

Figure 6. Some Internal Obstacles

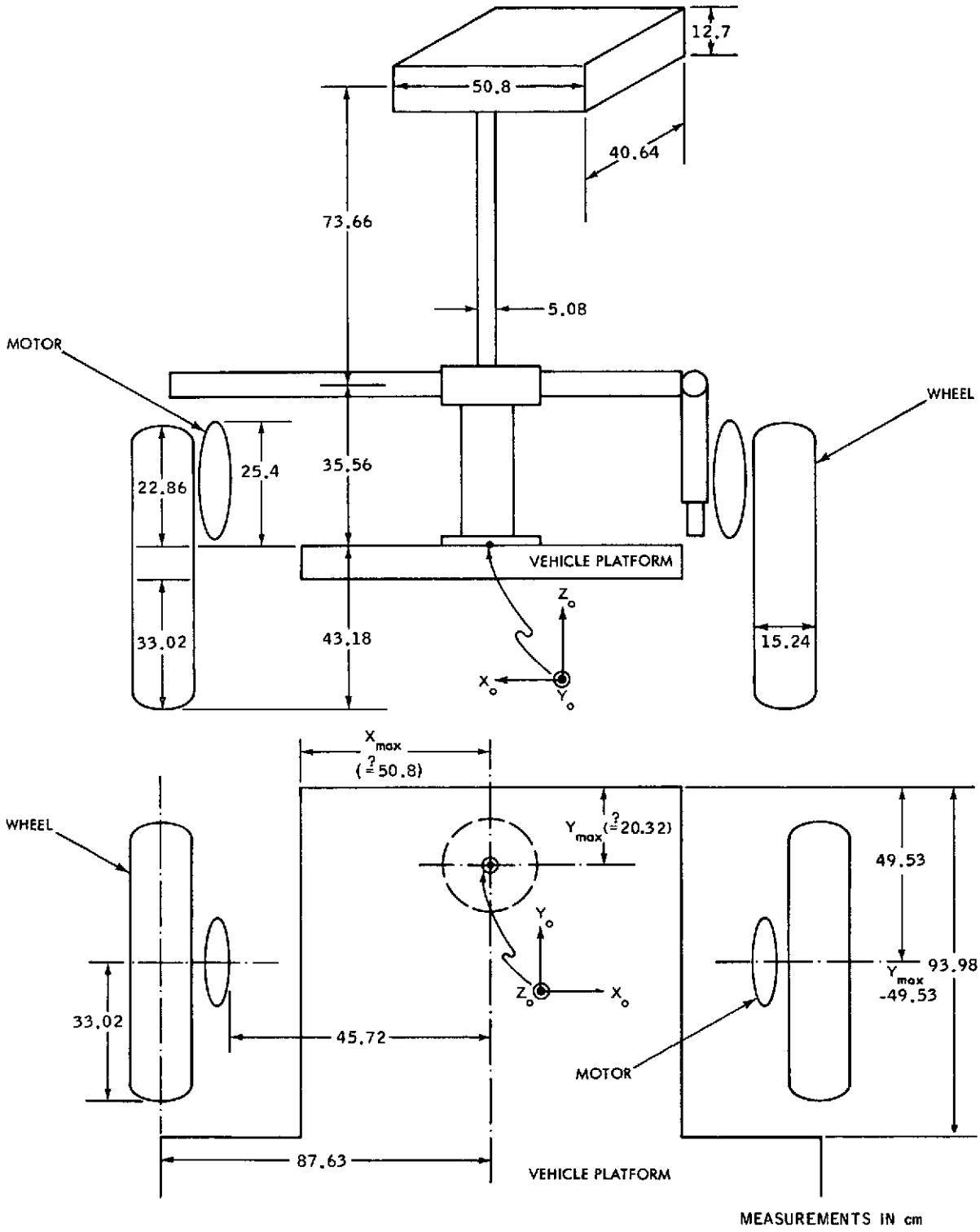

Fig. 7. Vehicular Obstacles

or an envelope of all possible positions can be used. In the case of the wheels and motors, it is assumed that the steering angle is always zero, that is, that the wheels point straight ahead such that the axis of wheel rotation is always along the manipulator base frame axis $\vec{x}_0$. Since the manipulator and the vehicle are not driven simultaneously, and since the vehicle wheels can be turned while the vehicle itself remains stationary, this constraint does not appear to be overly restrictive. In the event that this assumption proves to be too restrictive, then an envelope of all possible wheel/motor positions will be used. The envelope is only slightly larger than the volume consumed by a single position both because the area of inside wheel surface above the platform is small (the wheel axis being four inches below the platform) and because the steering angle is limited (perhaps to ±30 deg). Calculating the location of the occupied volume is considered undesirable and a nuisance; one of the purposes of categorizing some obstacles as permanent is to avoid numerous computations and to take advantage of simpler invariant collision checks that can be devised for permanent obstacles.

An envelope of all possible TV/laser positions has been selected for implementation over an assumed position because of the wide variability in the location of the occupied volume as the TV/laser head pans and tilts.

Environmental obstacles include items placed on the platform by the manipulator as well as such features as rocks, ground slopes, and surface holes.

If and when the robot breadboard becomes equipped with two manipulators that work together, then each manipulator becomes a nonpermanent (in fact, moving) obstacle to the other.

2. Detection of Permanent Obstacles

Joint limit violations are detected by evaluating each trajectory polynomial at its extreme values and comparing the extrema against the acceptable limits. Finding the extrema is particularly straightforward with cubics, as they are either at the endpoints or at the roots of the quadratic derivative of the trajectory cubic.

All other permanent obstacles are detected by evaluating the trajectories for the six joints at numerous (currently 21) points along the trajectory and

comparing the resulting sequence of link positions with the positions of the fixed obstacles.

Generally, collision testing of this type involves determining the distance between a link (i.e. a line with a link-radius and safety-radius added, forming a cylinder) and a point, line, or combination of lines (obstacle envelope edges). Computation is reduced considerably by the invariant geometry of the obstacles; numerous simple tests based on various joint variable values can be performed. In many cases, permanent obstacle detection is reduced to the task of evaluating certain simple inequalities.

Link equations and link distance formulas are given in Appendix 4.

3. Avoidance of Permanent Obstacles

Two general methods of obstacle avoidance are presented here, each of which is applicable to both permanent and nonpermanent (environmental) obstacles. The two approaches are referred to as "the freeway method" and "adding cubics".

The freeway method consists of the precomputation and storage in a data file of a number of trajectories relating commonly accessed arm positions/orientations. Various park positions, tool bin and rock box locations on the platform, manipulator positions and position sequences for presenting objects to the sensory subsystem, and perhaps some target locations on the ground are all commonly accessed points that can be related to each other by precomputed trajectories, i.e., freeways. Slight variations from these standard initial and terminal points can be dealt with using freeway entrance and exit trajectories.

The freeway method saves computer time and guarantees a safe path at the cost of more storage and somewhat reduced flexibility. Flexibility is retained using the addition of cubics method; with both implemented, the freeway method becomes a valuable adjunct.

Adding cubics is the other implemented obstacle avoidance procedure. Specifying an additional intermediate condition for a joint (position, normally, although other intermediate conditions can be used) and an additional trajectory segment time, one can add a cubic such that the resulting trajectory satisfies all the original constraints as well as the new one. By partitioning an original trajectory segment time, the trajectories and the times for the other joints and

for the preceding and terminal segments of the modified-trajectory joint need not be changed; hence only a few coefficients require recomputation. Adding a cubic is achieved by repeated application of the relationships in Table 4 of Appendix 3.

In the planning of obstacle avoidance maneuvers, either planning control or execution control of the trajectory can be implemented. Planning control assumes poor accuracy during execution time; obstacles are avoided by using large safety margins and leaving room for large errors. In execution control, it is assumed that fairly high positional accuracy is achieved in executing a trajectory and thus only small safety margins are required. For the JPL manipulator, it is expected that no point on any link will ever be more than 1.27 cm from where it was planned to be and, in general, will be much closer than that. Thus very small safety margins are used. Details of detection and avoidance of specific permanent obstacle are provided in a series of JPL internal documents.

4. Detection and Avoidance of Nonpermanent Obstacles

Nonpermanent obstacles can be detected and avoided in the same general ways as indicated above for permanent obstacles. Furthermore, careful selection of approach direction and final hand orientation can be of use. There are two additional considerations in avoidance. First, it can be assumed that, in the real world, out of doors, obstacles rest on the ground and hence can be avoided by going over them. Second, a type of reflexive obstacle avoidance (applicable as well to the task of aiding the coordinated motion of two arms) is possible using sensors of the type described in Ref. 10.

IV. DYNAMICS

In this section, some dynamic considerations impacting planning program implementation are presented. The equations of motion of the arm are given (based on Ref. 5) and kinematic-dependent coefficient matrices are separated from time-dependent factors in the equations of motion (as in Ref. 6) in order to derive several computation-reducing relationships. Sample trajectories are used to compare the effects on computed generalized force of several approximations. Finally, a brief discussion of forces and moments with an example application to the task of weighing objects is given.

A. Equations of Motion and Coefficient Matrices

The equations of motion for the manipulator can be expressed (See Appendix 5) as

$$F_i = C_i + \sum_{k=1}^{6} C_{ik}\,\ddot{q}_k + \sum_{k=1}^{6}\sum_{m=1}^{6} C_{ikm}\,\dot{q}_k\,\dot{q}_m, \quad i=1\ldots,\ 6,$$

where F_i is the generalized force (force for joint 3, torque for the other five joints) applied to joint i, q_i is the i^{th} joint variable (r_3 for joint 3, θ_i for the other joints), and the C's are the time-independent (but joint position dependent) coefficients defined in Appendix 5.

The first term, C_i, describes the effect of gravity on link i. The second set of terms describes the reaction force on link i of the acceleration of link k (if $k \neq i$) or the force required to accelerate the link and overcome motor (i.e. rotating) inertia (if k=i). The third set of terms describes the centrifugal (k=m) and Coriolis ($k \neq m$) analogs for the arm, the effects on link i of the coupled velocities of links k and m.

Only 83 of the 258 coefficients need be computed; the rest are determined from the following (proven in Appendix 6):

1. $C_{ik} = C_{ki}$
2. $C_{ikm} = C_{imk}$
3. $C_{i3m} = 0, \quad m \geq 3$

4. $C_{ikm} = -C_{mki}$, $i, m \geq k$ $\left[\Longrightarrow C_{iki} = 0,\ i \geq k,\ \text{and } C_{kkk} = 0\right]$

5. $C_1 = 0$ if the arm-relative gravity vector is vertical.

The first statement indicates that the reaction force coefficient for link i due to the acceleration of link k is the same as the coefficient for link k due to the acceleration of link i.

The second statement follows directly from the equations of motion.

The third statement indicates the lack of interactive effect on any joint of the boom (link 3) velocity and the three wrist link velocities.

The fourth statement demonstrates the reflexive interaction of outer links' (i and m) velocities as they couple with the velocity of an inner link k. Also, there is no interactive effect on any outer link due to coupling of its own velocity with that of any inner link, and, in addition, no joint feels any of the radially-directed centrifugal effects of its own motion.

The fifth statement indicates that joint 1 feels no gravity effects when the first link is vertical.

Each time it is desired to determine the nominal applied force/torque F_i, then only 83 joint position dependent coefficients need be computed. It is useful to know how many times these coefficients need be recomputed over a whole trajectory.

B. Generalized Force Over Trajectories

Consider the two sample trajectories described in Fig. 8. In the first, the arm moves from a left arm park position with extended hand and horizontal boom up 7.5 cm; then down to a spot 7.5 cm above the ground and 56 cm in front of the vehicle and finally down to the ground. The second trajectory moves the arm from the latter position to a point on the vehicle platform 89 cm behind the arm post. Both trajectories are in three parts, one for liftoff, one for the major motion, and one for setdown, and have been computed with five cubics.

The time histories of the generalized force vector $\vec{F}$ over the two trajectories have been plotted in Figs. 9 and 10. For each joint and for each trajectory four curves are plotted, one each showing the contribution of the gravity term (the curves labelled "G"), the velocity terms ("V"), the acceleration terms ("A") and the total force or torque ("F").

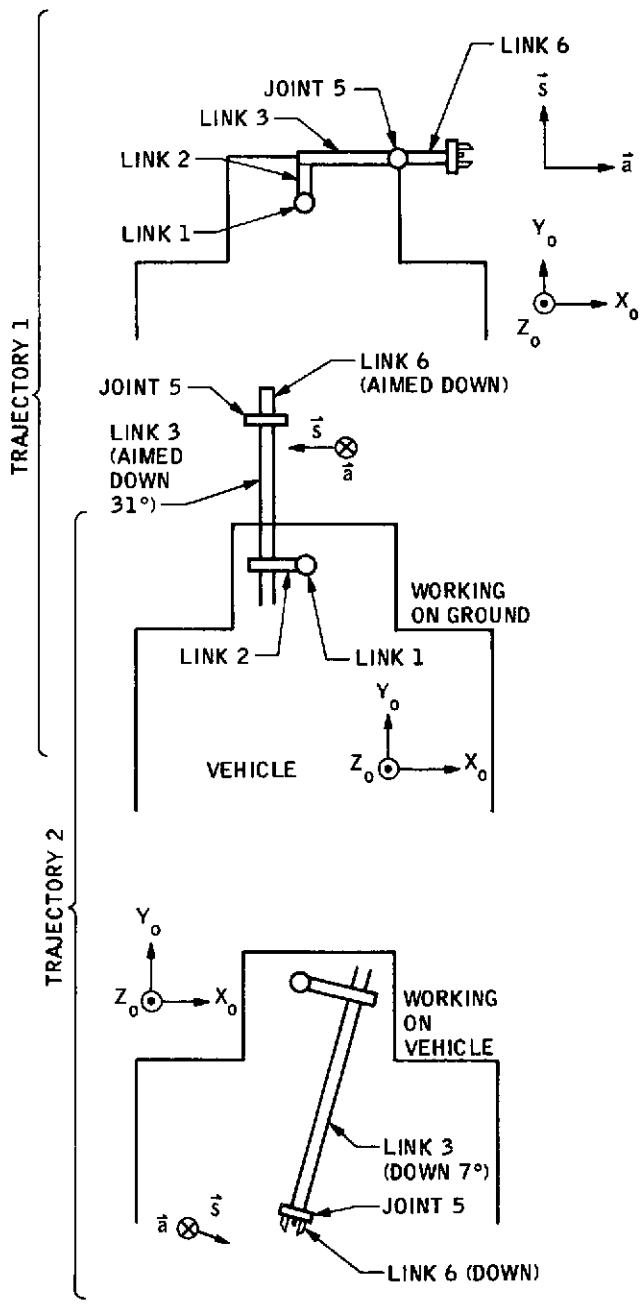

$\vec{\theta}_0$ = (0°, 90°, 26 cm, 0°, 0°, 0°)

to $\vec{\theta}_1$ = (0°, 74°, 27.1 cm, 0°, 16°, 0°)

to $\vec{\theta}_2$ = (90°, 121°, 89 cm, 90°, 59°, 0°)

to $\vec{\theta}_3$ = (90°, 125°, 94 cm, 90°, 55°, 0°)

TRAJECTORY 2: from $\vec{\theta}_3$ to $\vec{\theta}_2$

to $\vec{\theta}_4$ = (-100°, 92°, 86 cm, 90°, 88°, -105°)

to $\vec{\theta}_5$ = (-100°, 97°, 89 cm, 90°, 83°, -105°)

Fig. 8. Arm Positions for Sample Trajectories

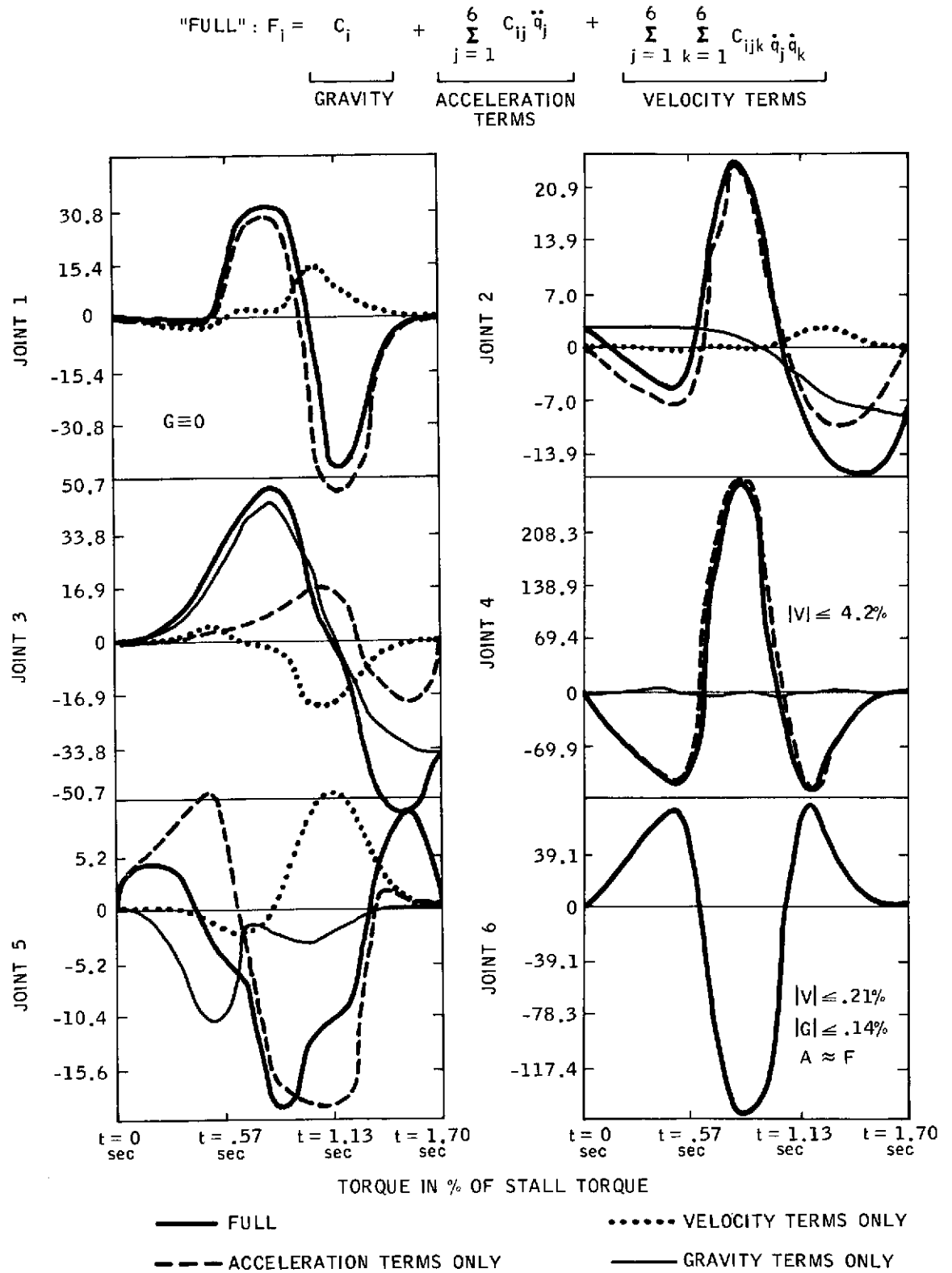

Fig. 9. Trajectory 1 Torque/Force Components

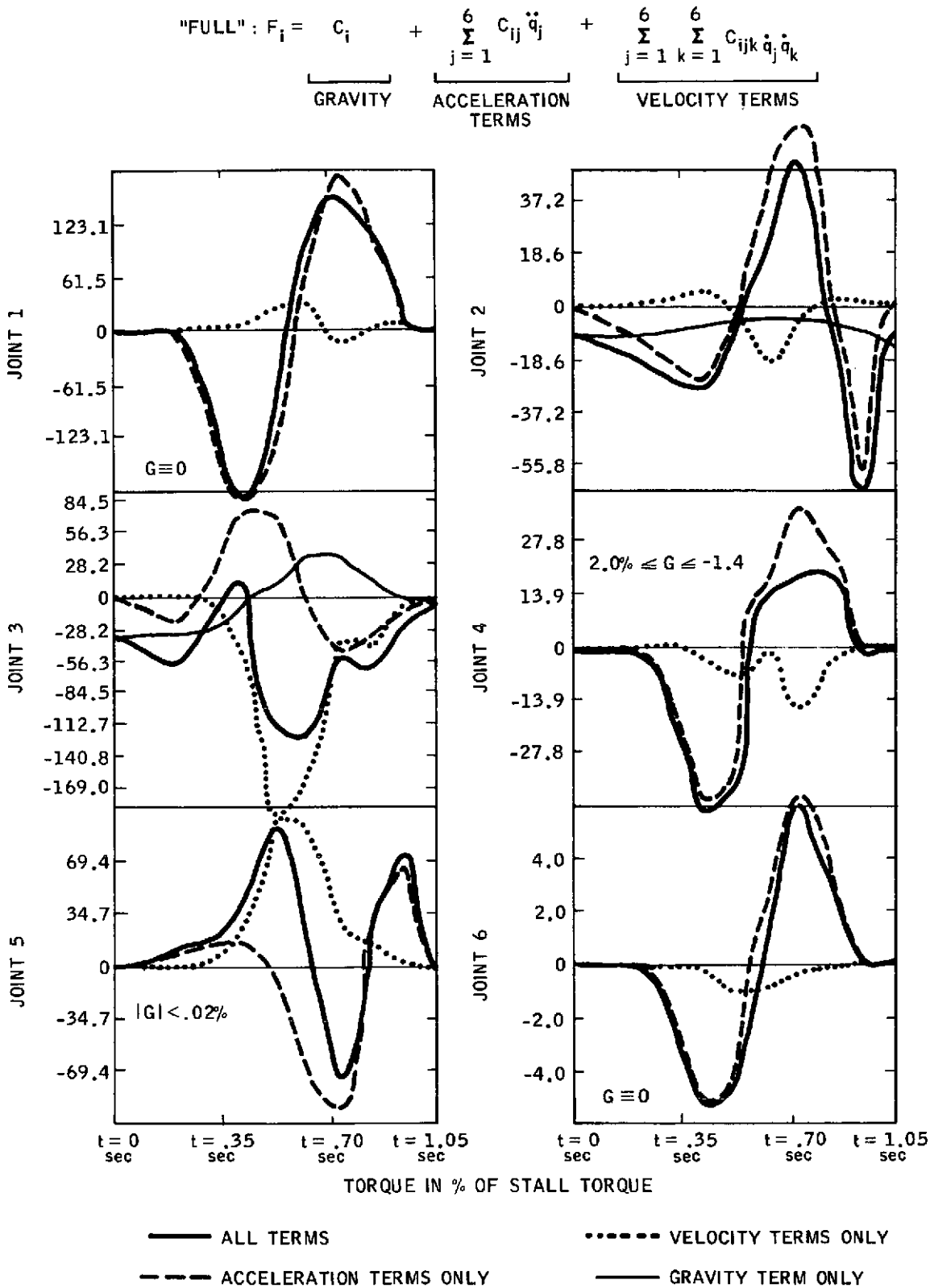

Fig. 10. Trajectory 2 Torque/Force Components

Joint 1 feels no gravity effects (vehicle assumed level). Almost all of the total torque required for the joint for the two sample trajectories is due to the acceleration terms; the velocity term are only significant briefly. Joints 4 and 6 also display this tendency. In fact, the inertial terms (i.e., those of the form $C_{ii}\ddot{q}_i$) clearly dominate the off-diagonal reaction acceleration terms, especially when the joint in question is being driven. (Recall that the diagonal coefficients C_{ii} include the very large motor inertias.)

In both trajectories, joint 2 also experiences high acceleration terms relative to total torque, with moderate contributions from the velocity terms. However, for joint 2, gravity is often significant and tends to separate the acceleration torque and total torque and total torque curves.

Joints 3 and 5 frequently experience large contributions from all three sources, as shown.

While it is true that of the 258 coefficients, only 82 or 83 need be computed, the questions remain as to how frequently they should be recomputed and how many of them (and which ones) should be recomputed. It is beyond the resources of the realtime computer to recompute all 83 60 times each second while still performing other operations.

Figures 11 and 12 begin to address these questions. In these figures, the curves labeled I represent the errors arising from interpolating the coefficients between the interpolation points indicated on the time scale. These interpolation points are at the beginning and end of the trajectory departure and arrival segments. If F is the fully computed force/torque ($= F(C_i, C_{ij}, C_{ijk})$) and $\hat{F}$ is the interpolated force/torque curve ($\hat{F} = F(\hat{C}_i, \hat{C}_{ij}, \hat{C}_{ijk})$), then the curve labeled I is given by $F - \hat{F}$. Thus the correct torque F to apply,

$$F = \hat{F} + I,$$

is comprised of a nominal torque $\hat{F}$ (coming from the plan) and an error torque I (coming from the control system).

The curves labeled II describe the interpolation error when all velocity terms are ignored. The curves labeled III only consider gravity and inertial acceleration terms, interpolated. The latter two interpolations have been used successfully in the Stanford Hand-Eye Project, the occasionally large errors for these approximations notwithstanding.

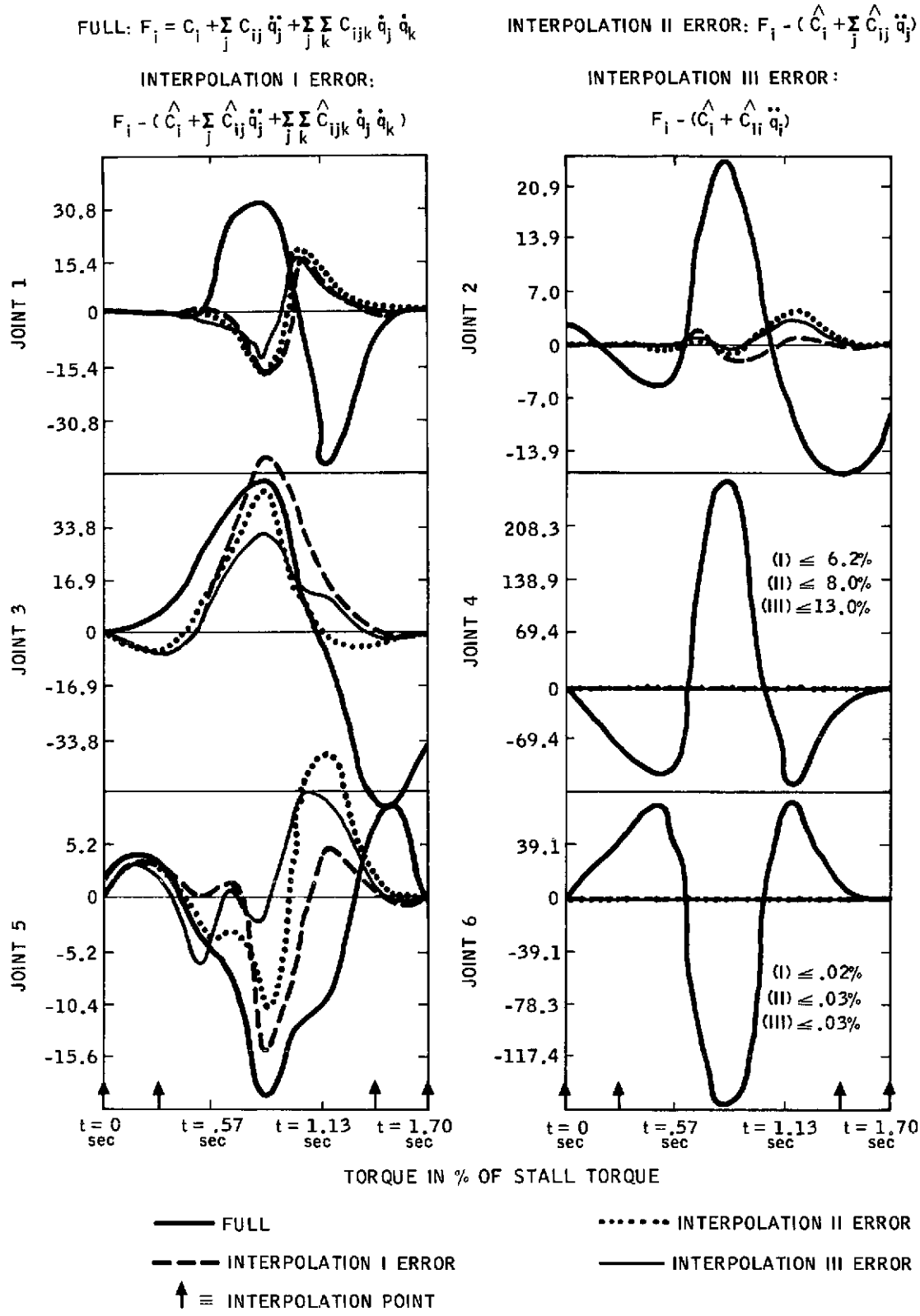

Fig. 11. Trajectory 1 Interpolation Errors

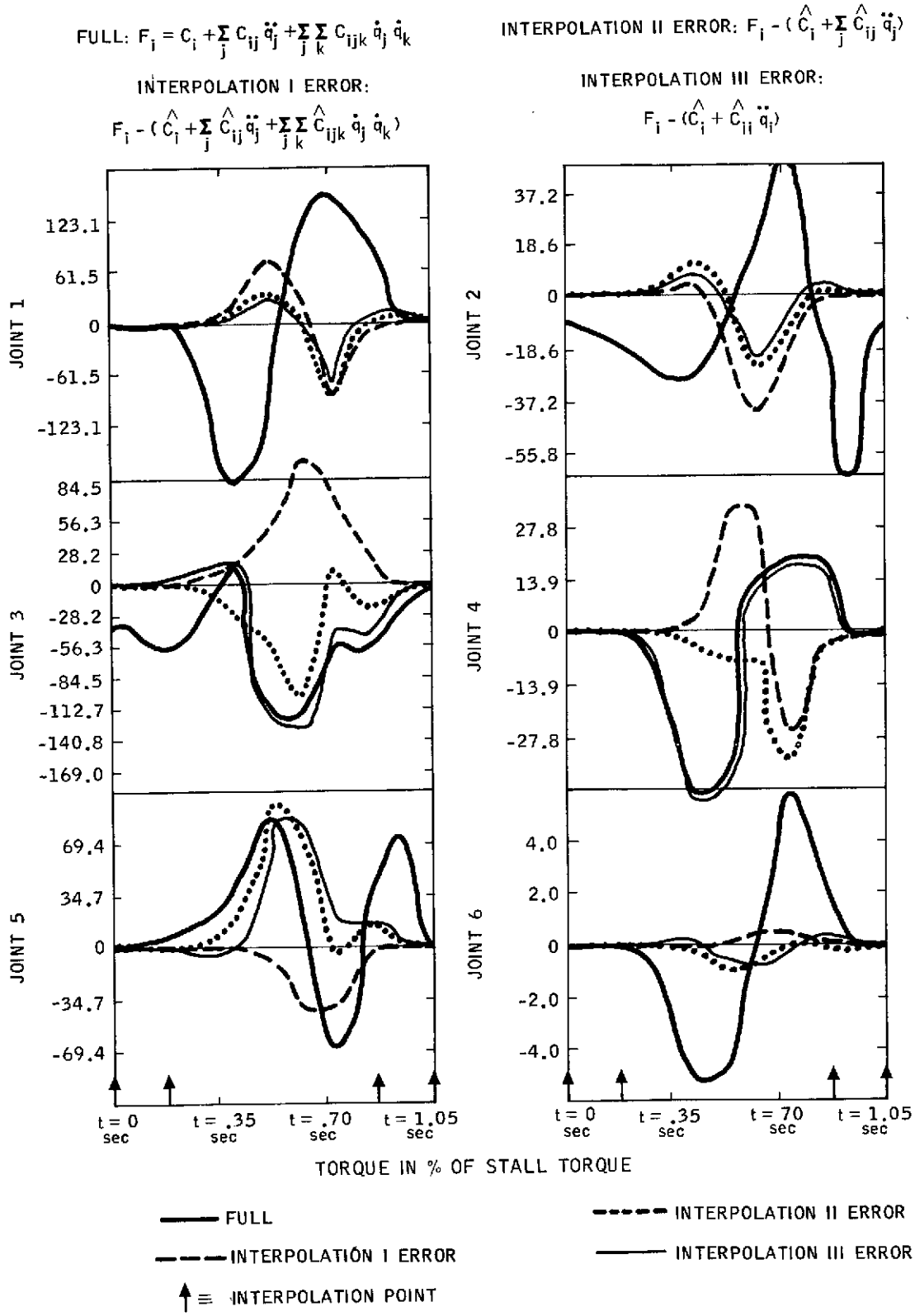

Fig. 12. Trajectory 2 Interpolation Errors

These trajectories are extremely rapid, requiring only 1.70 and 1.05 seconds, respectively. Doubling the trajectory times (to 3.40 and 2.10 seconds) cuts all components of all the curves of Figs. 9, 10, 11, and 12 by a factor of 4, with the exception of the gravity curves and gravity components. This two to three second trajectory time is more representative. Plots for interpolation III and full torque for joint 5, both trajectories, appear in Fig. 13 with original and doubled times compared.

It is desired to reduce the approximation and interpolation errors both in absolute terms and relative to the actual desired torque F. Adding an additional interpolation point in the middle of the mid-trajectory segment gives the error curves plotted in Figs. 14 and 15 (original time scale). Note that the error torques for joints 3 and 5 are still especially large.

Most of the error remaining in the error curves comes from neglecting the centrifugal terms $C_{ijj}\dot{q}_j^2$ for j = 1, 2, 4, 5. (Recall that $C_{i33} = 0$.) Adding these terms back yields the quite acceptable error curves IV plotted in Figs. 16 and 17. For comparison, the full torque curves are plotted.

Finally, in Figs. 18 and 19, these same curves are plotted with doubled times (two to three seconds), accurately reflecting currently planned trajectory times. The vertical scale in these figures indicates the nominal, error, and full torques relative to the limit for each joint. Observe that in neither trajectory does any joint come very close to the limit, and, in fact, the applied torque will rarely exceed 25% of the limiting values. Note further that with the two to three second trajectory, the nominal torque $\hat{F}$ is generally quite close to the desired torque; IV = F - $\hat{F}$ is small. Finally, it is noted that the computations required in implementing this approach are well suited to minimizing computer-to-computer communication buffer size and to an efficient allocation of activity between the planning computer and control computer.

C. Forces and Moments

Ref. 6 describes the effects of applying a force $\vec{F}_0 = (f_x, f_y, f_z, 0)$ and moment $\vec{M}_0 = (M_x, M_y, M_z, 0)$ to the end of the hand. ($\vec{F}$ and $\vec{M}$ expressed in base reference system, as indicated by the subscripts.) In hand coordinates,

$$\vec{F}_6 = T_6^0 \vec{F}_0 \qquad \text{and} \qquad \vec{M}_6 = T_6^0 \vec{M}_0$$

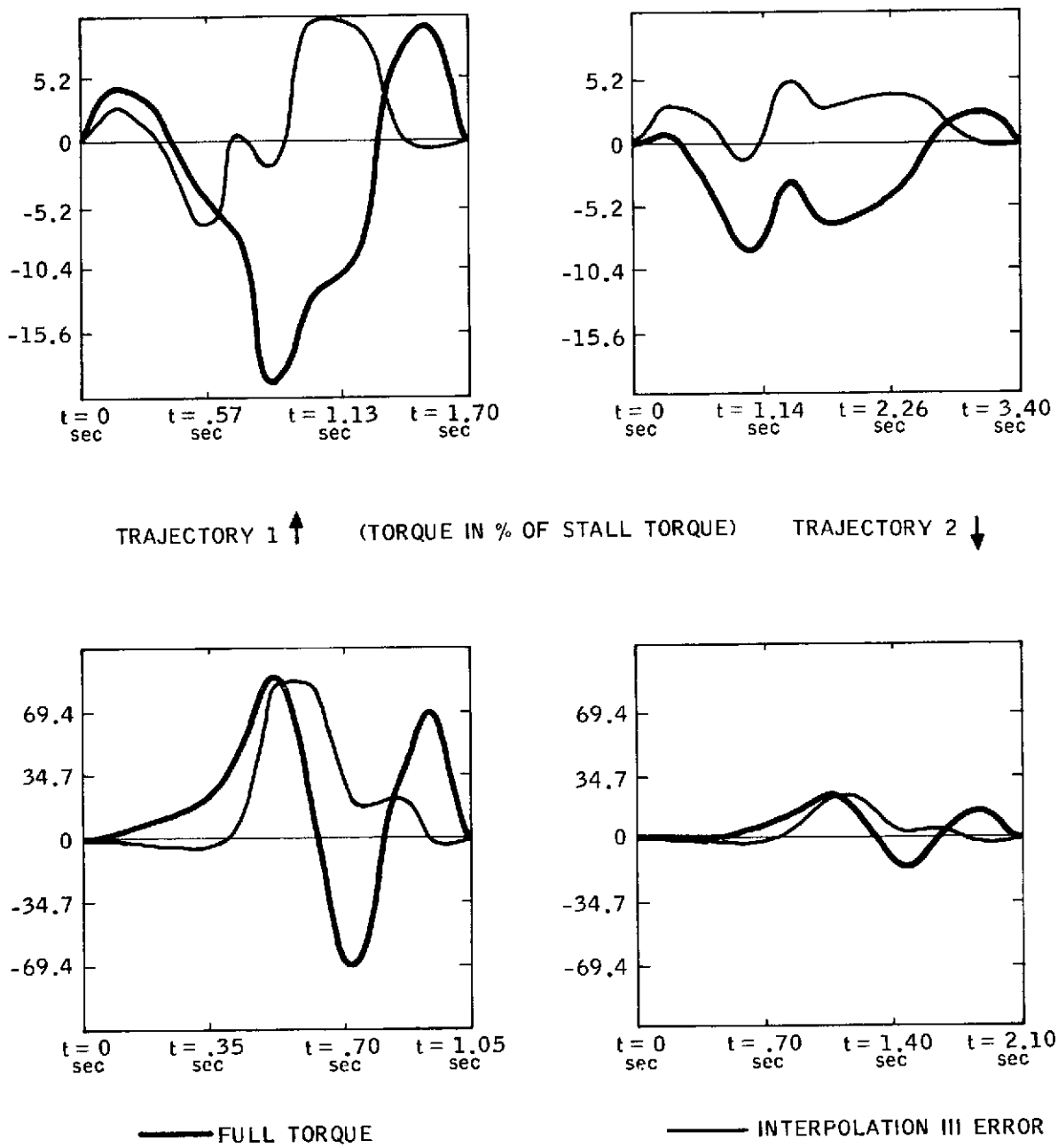

Figure 13. Joint 5 Interpolation III Errors: Effects of Doubling Time

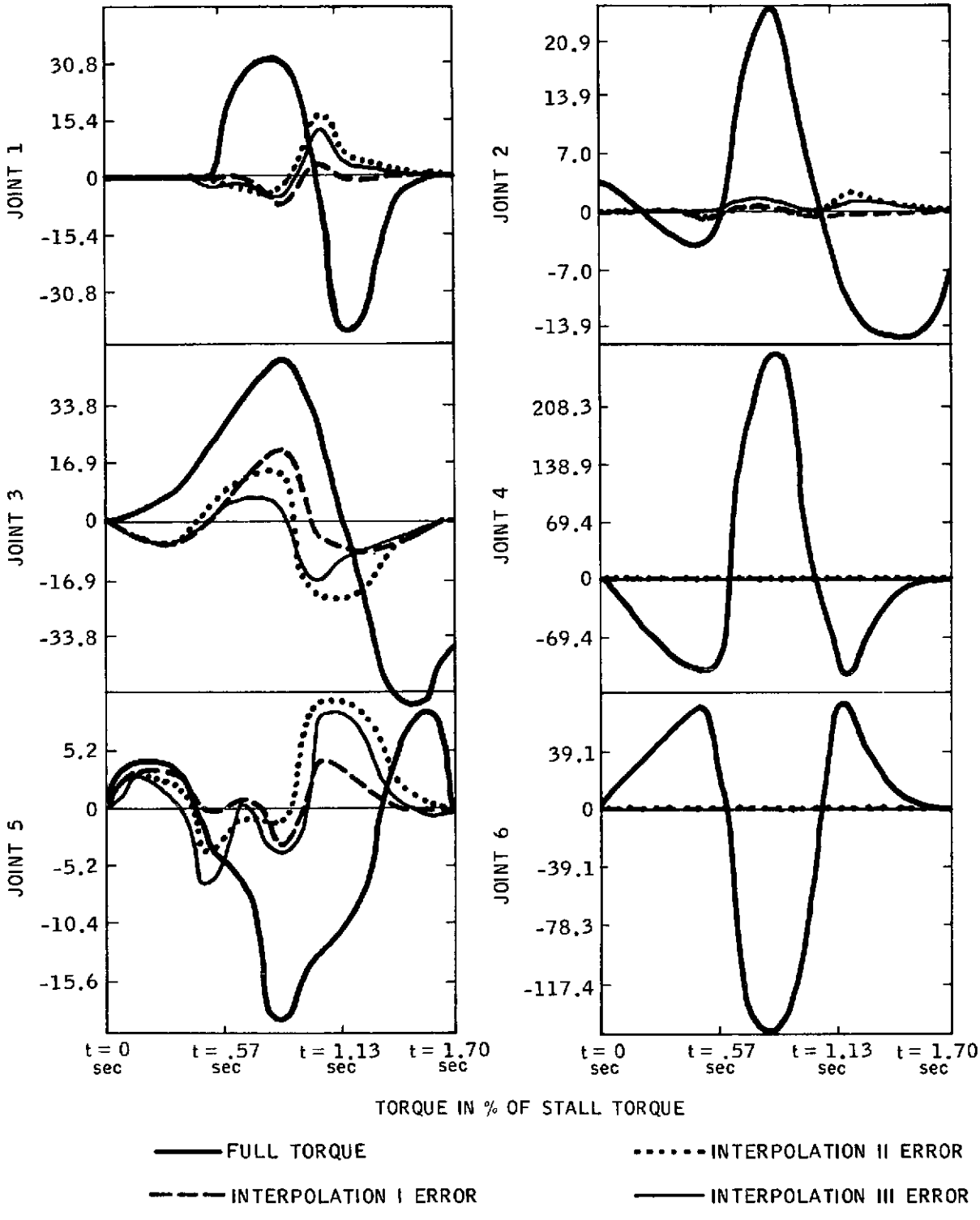

Fig. 14. Trajectory 1 Interpolation Errors with Midpoint Interpolation

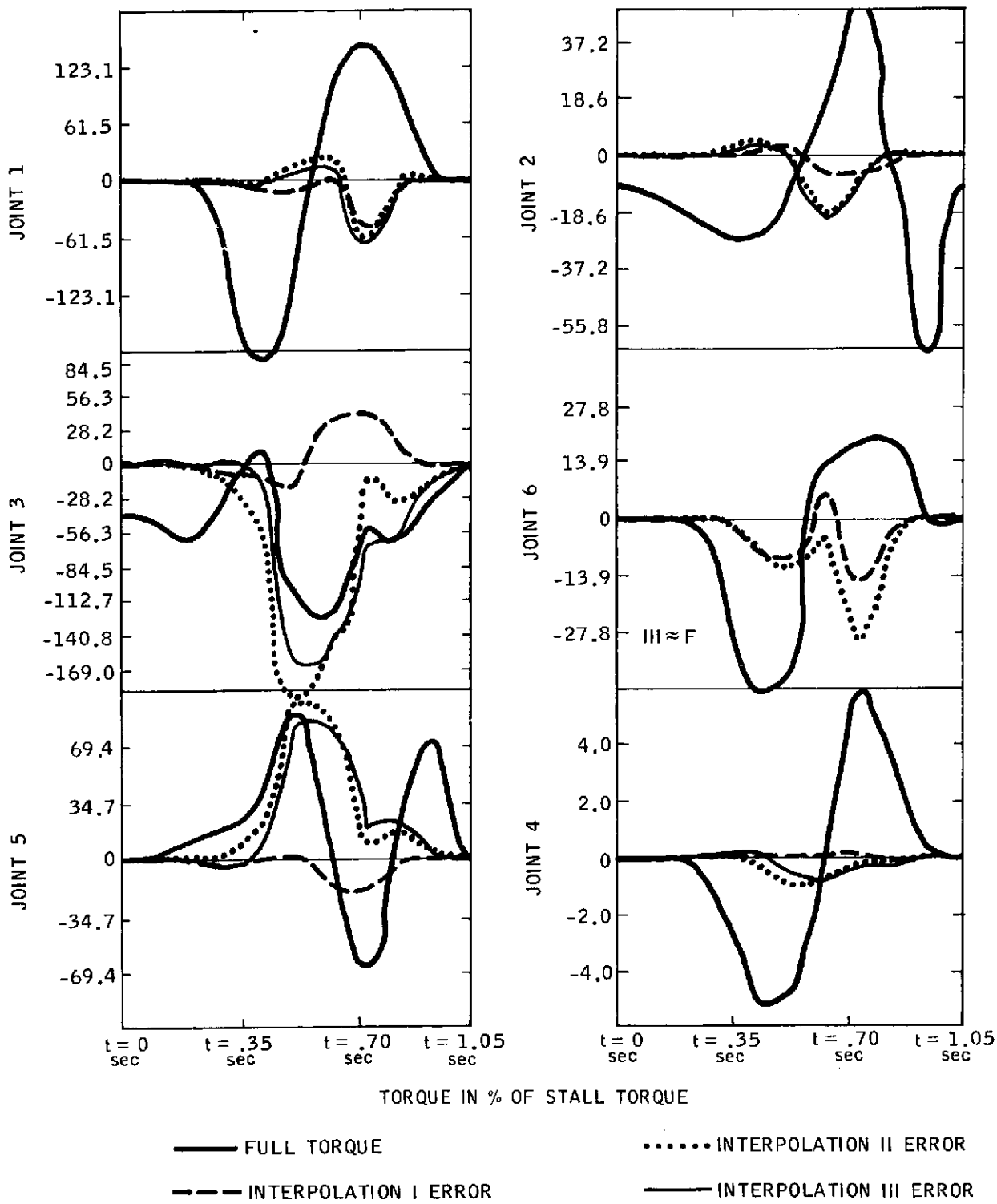

Fig. 15. Trajectory 2 Interpolation Errors with Midpoint Interpolation

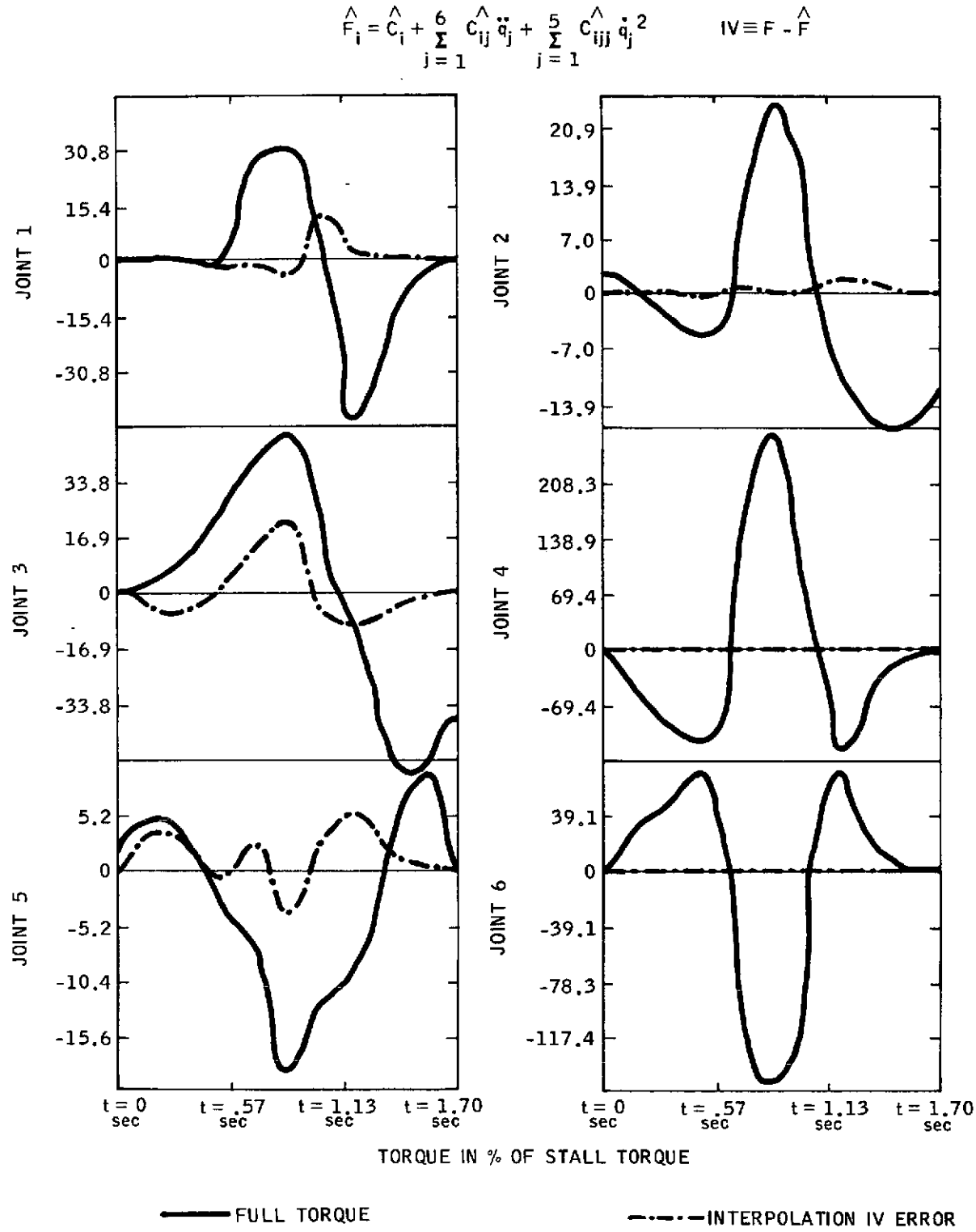

Fig. 16. Trajectory 1 No Coriolis Interpolation Error

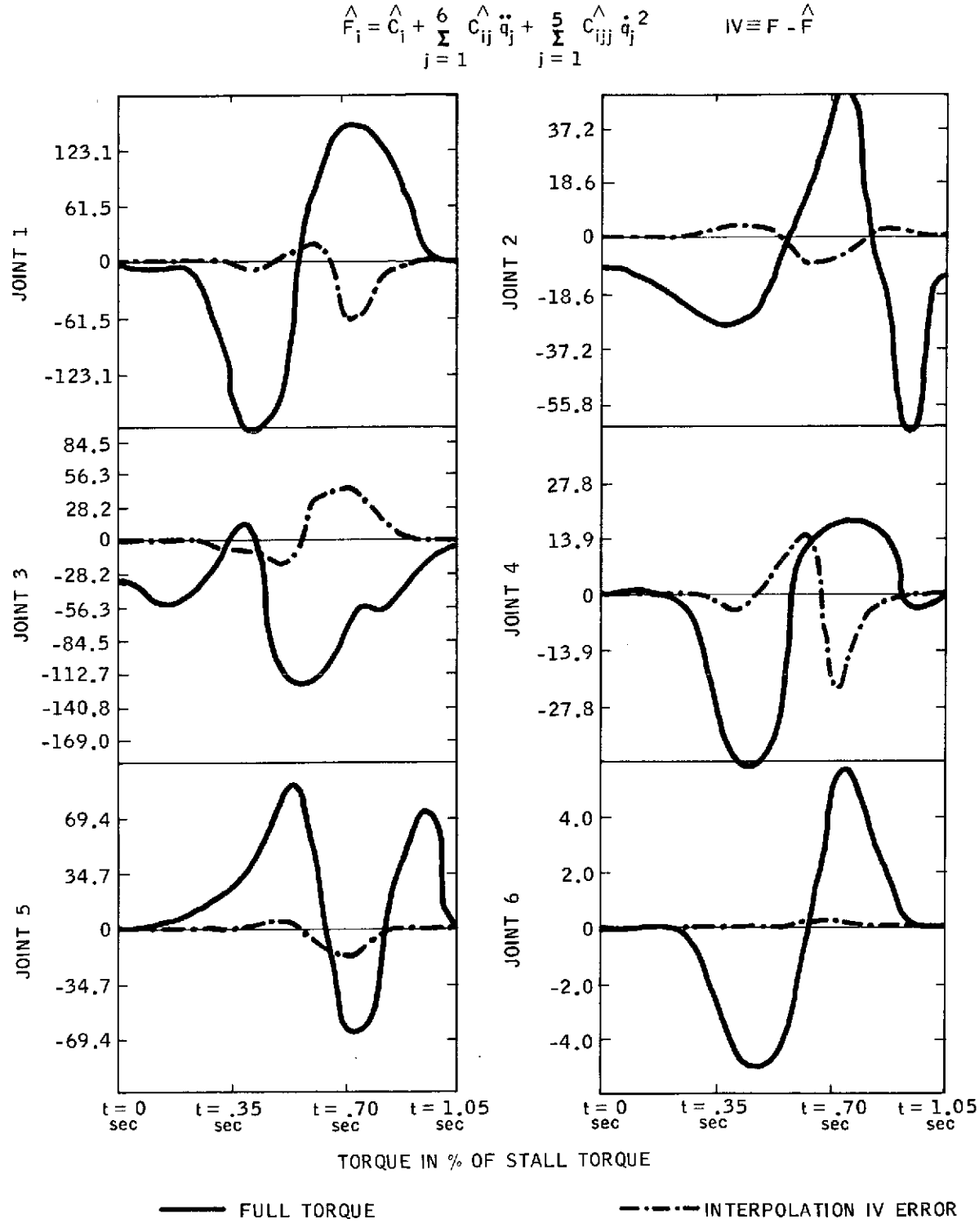

Fig. 17. Trajectory 2 No Coriolis Interpolation Error

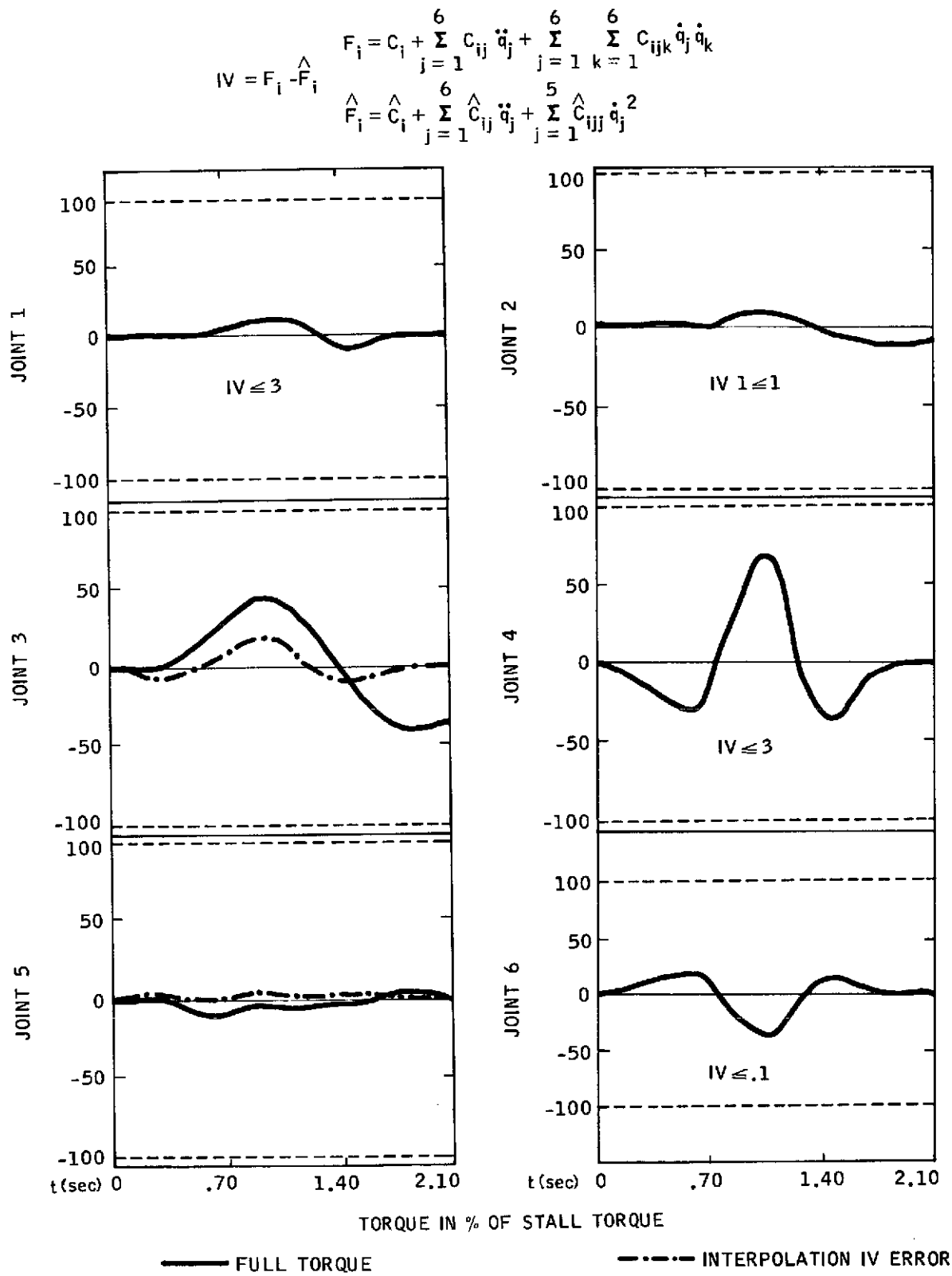

Fig. 18. Trajectory 1 Actual Torque and Error Torque

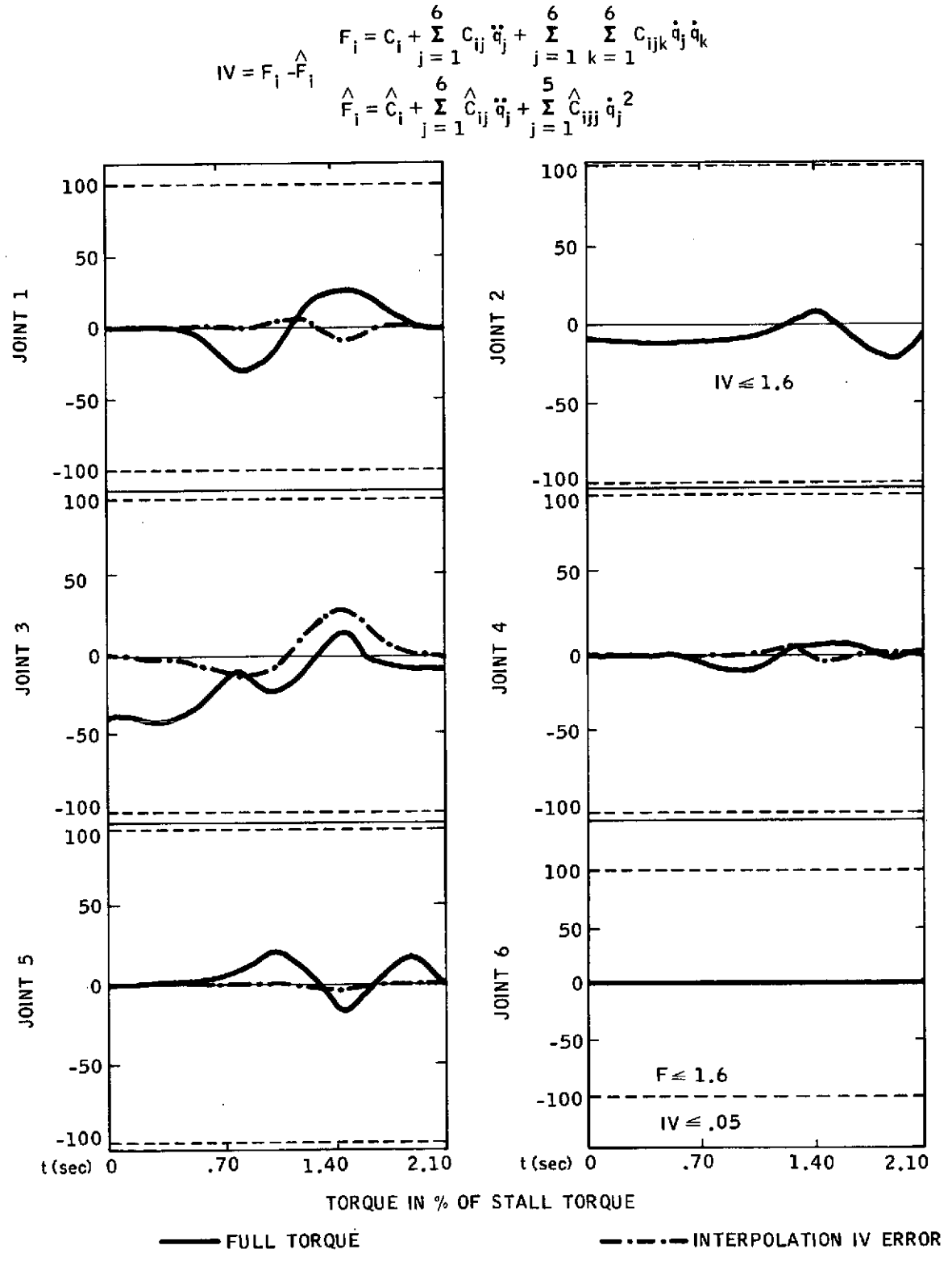

Fig. 19. Trajectory 2 Actual Torque and Error Torque

The forces and moments felt at the other joints are given by

$$\vec{F}_{j-1} = T^{j}_{j-1}\,\vec{F}_{j} = T^{0}_{j-1}\,\vec{F}_{0} \qquad , j = 1, \ldots, 6 \tag{19}$$

$$\vec{M}_{j-1} = T^{j}_{j-1}\,\vec{M}_{j} + \vec{P}_{j} \times \vec{F}_{j-1} \qquad , j = 1, \ldots, 6, \tag{20}$$

where

$\vec{P}_j$ = column 4 of T^{j}_{j-1}.

The reaction torque is the negative of the third component of $\vec{M}_j$ if joint j is revolute; the reaction force is the third component of $\vec{F}_j$ if joint j is prismatic (i.e., if j = 3). The third component is the one acting in the $\vec{z}_i$ direction, the line of action for joint i + 1. The reaction vector consists of five reaction torques and one reaction force (for joint 3).

Suppose a 1 kg rock is enclosed in the hand as the arm lifts and then stops. Assuming the vehicle to be gravitationally horizontal, we can compute the reaction vector $\vec{R}$ for

$$\vec{F}_0 = \begin{bmatrix} 0 \\ 0 \\ -1 \\ 0 \end{bmatrix} \quad \text{and } \vec{M}_0 = \vec{0} \text{ as } \vec{R} = -\begin{bmatrix} 0 \\ r_6(s_2c_5 + c_2s_{45}) + r_3s_2 \\ -c_2 \\ r_6s_{25}c_4 \\ r_6(s_{24}c_5 + c_2s_5) \\ 0 \end{bmatrix}$$

The error torque set up when a rock is lifted can be compared to the above reaction vector $\vec{R}$ for a 1 kg rock to obtain the weight of the rock. By keeping the arm unbraked and motionless, error torques that are free from the approximation effects of the previous section can be read.

V. SOFTWARE

The manipulator software fits into the overall robot system software structure as indicated in Fig. 20. An operator provides goals to either the robot executive (REX) or the time-shared computer manipulator programs (TSCMP's). In either case, the communication is mediated by the Master Control Program (MCP).

The Robot Executive consists of three parts: a cognitive executive, which plans activities by sequencing and combining the planning activities of individual robot subsystems (i.e. manipulator, vehicle, TV/laser rangefinder); a world model into which the resulting subsystem plans, state of the robot, and state of the world are stored; and an operating executive, responsible for execution of the planned activities.

The TSCMPs can likewise be considered as being comprised of three program groups: a group of "up-interfacing" programs which serve to decode commands to the arm and sequence specific-motion planning activities; a group of planning programs which compute trajectories, torques, and other quantities (as partially described in the preceding sections); and a group of "down-interfacing" programs which code the results of planning program activity for the RTC.

Operator or cognitive executive-generated plans start the TSCMP's. The packed buffers (see below) representing the plan are then either returned to the cognitive executive for naming and storage in the world model, or they are directly transmitted by the TSCMP's to the RTC. In the latter case, RTC feedback goes back to the TSCMP's and then, after processing, to REX. In the former case, the operating executive selects the appropriate buffer(s) (i.e. plan) from the world model and transmits them to the RTC, in which case RTC feedback goes to the TSCMP's indirectly.

The world model is capable of storing plans and robot-environment states. The TSCMP's also include a permanently maintained data file for the storage of frequently accessed manipulator data (i.e. the "freeways" of Section IIIC3).

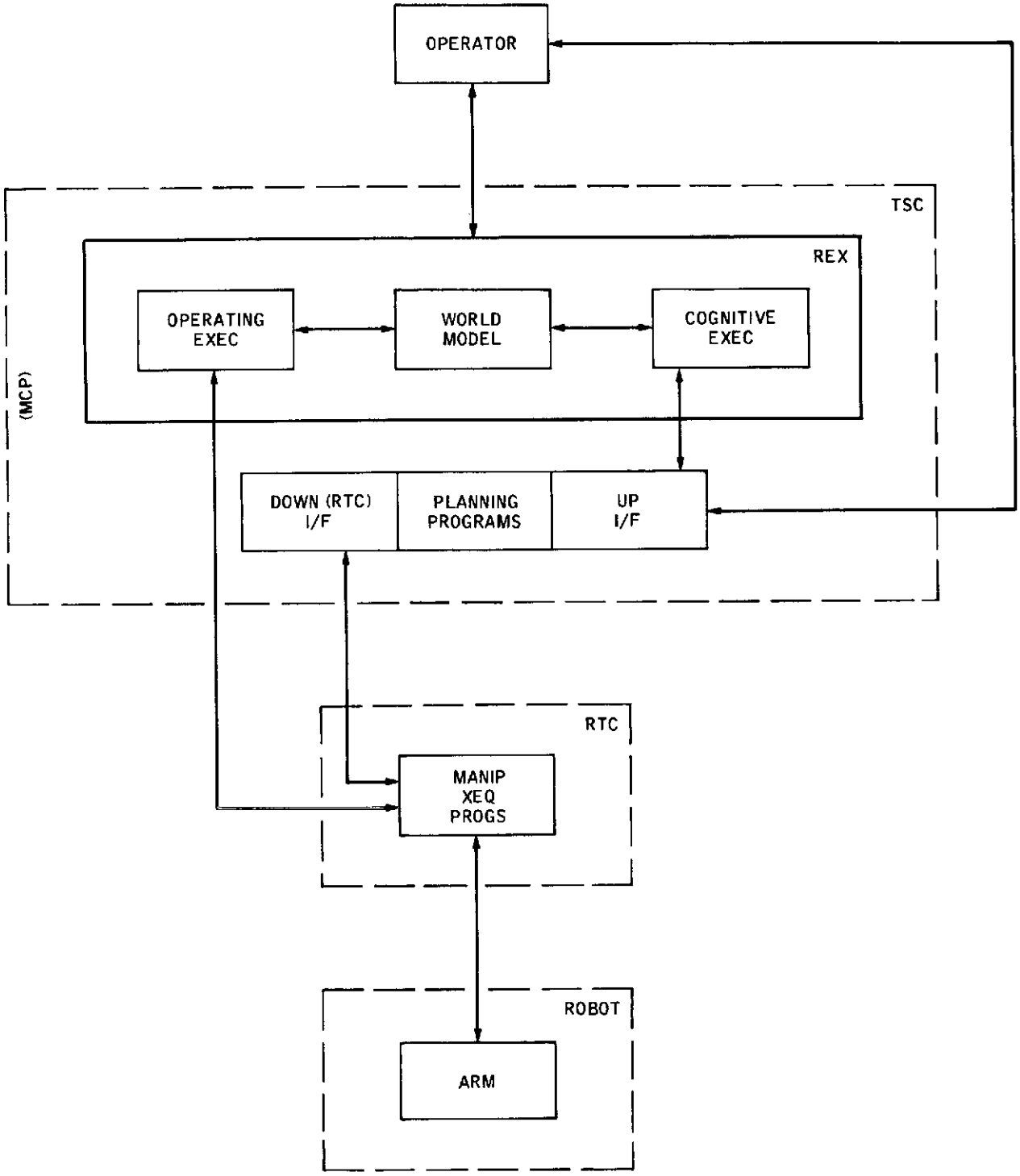

Figure 20. Manipulator Software in Robot System

Plans developed in the TSC for the manipulator are coded for the RTC into one or more 2048 word 16-bit buffers. The buffers can be arranged into separate and complete groups, with sequencing within and between groups. Each individual buffer is organized into three parts: a header, a control stack, and an argument list. The header contains data pertaining to the sequencing of buffers. The control stack contains the sequence of specific commands to be executed and, for each command, a pointer to a place in the argument list where parameters of the command are to be found. Samples of currently implemented functions (i.e. control stack entries) are provided in Appendix 7.

Commands from above (i.e. from REX or the operator) are of four types. Bookkeeping commands affect the permanent arm data file and serve to define, name, store, delete, and retrieve data. Status commands are requests for output either to the operator or to REX. Planning commands result in the filling of RTC-bound buffers; examples include moving the arm, opening and closing the hand, exerting a force, and moving a single joint, as well as other commands. The fourth command type, execution commands, affect the RTC, causing the RTC to read, clear, or execute buffers.

As an example of manipulator software functioning, consider the following. An operator provides a high-level command to retrieve a green rock. The cognitive executive initiates first TV/laser rangefinger planning activity, then vehicle motion activity; after these two plans are executed and another TV/laser plan is formulated and executed, the rock is located as being within reach of the arm. A "MOVE" command is given to the TSCMP's. Programs performing the computations described in the above sections then determine the joint variables required for the hand to grasp the rock, compute a five-cubic trajectory for each joint to bring the arm to that position, and compute five sets of coefficient matrices for the equations of motion. Possibly more than five cubics are required for some joints, if obstacles are present. The polynomial coefficents and coefficient matrices are packed into the argument list, and hand opening, trajectory, and hand closing entries are packed into the control stack. The buffer is transmitted to the RTC where each cycle the polynomials and coefficient matrices are used to compute nominal torques for each joint. To these nominal torques are added correction terms, and then these resultant torques are converted into current for transmission to the motors of the arm. Upon completion of the task, summary feedback is returned to the TSCMP's and the cognitive executive or operator.

VI. CONCLUSIONS

The relationships governing the planning and implementation of specific arm motions have been summarized. The incorporation of the resulting manipulator software into an effective robotic appendage will require conditional planning and perhaps use of the full sensory capabilities of the manipulator.

Conditional planning is currently being considered for implementation with proximity sensors, light-emitting diodes capable of providing direct range information. Addition of proximity sensors (Ref. 10) will enable the links of the arm to maintain a minimum safe distance from sensed obstacles without planning program intervention. Arm-mounted proximity sensors can also supplement TV/laser range finder data about the external environment.

The arm has internal position and rate sensors. In addition, force can be implicitly sensed by monitoring motor currents. Tactile and proximity sensing and the possible future addition of an adaptive hand provide further sensory capabilities. Thus the arm can be used as a science instrument, possibly in real-time interaction with other sensors, in addition to its use as an effector. For instance, rocks can be weighed, external dimensions estimated, approximate densities determined, and perhaps even crude rock identifications made.

Manipulator software efforts are currently directed towards the development of RTC software (Ref. 11) and the unification of TSC, RTC, and arm into a single system. Subsequent efforts will be directed towards the implementation of conditional planning and its integration with the already implemented deterministic planner, after which the sensory capabilities of the manipulator and its associated hardware are to be explored and exploited.

REFERENCES

1. Scheinman, V. D., "Design of a Computer Controlled Manipulator," Artificial Intelligence Memo 92, Stanford Artificial Intelligence Project, Stanford University, June, 1969.

2. Dobrotin, B. M., Scheinman, V. D., "Design of a Computer Controlled Manipulator for Robot Research," Third International Joint Conference on Artificial Intelligence, Stanford University, August, 1973.

3. Hartenberg, R. S. and Denavit, J., Kinematic Synthesis of Linkages, McGraw Hill, New York, N. Y., 1964.

4. Uicker, J. J., Hartenberg, R. S., and Denavit, J., "An Iterative Method for the Displacement Analysis of Spatial Mechanisms," Journal of Applied Mechanics, June, 1964.

5. Uicker, J. J., "On the Dynamic Analysis of Spatial Linkages Using 4X4 Matrices," PhD Thesis, Northwestern University, 1965.

6. Paul, R. C., Modeling, Trajectory Calculation, and Servoing of a Computer Controlled Arm, PhD thesis, Stanford University, August 1972.

7. Kahn, M. C., "The Near-Minimum-Time Control of Open-Loop Articulated Kinematic Chains," Artificial Intelligence Memo 106, Stanford Artificial Intelligence Project, Stanford University, December 10, 1969.

8. Pieper, D. L., "The Kinematics of Manipulators Under Computer Control," Artificial Intelligence Memo 72, Stanford Artificial Intelligence Project, Stanford University, October 24, 1968.

9. First Annual Report for the Development of a Multi-Moded Remote Manipulator System, Charles Stark Draper Laboratory, MIT, January 10, 1972.

10. Johnston, A. R., "Optical Proximity Sensor for Manipulators," Technical Memorandum 33-612, Jet Propulsion Laboratory, May 1, 1973.

11. Markiewicz, B. R., "Analysis of the Computed Torque Drive Method and Comparison with Conventional Position Servo for a Computer-Controlled Manipulator," Technical Memorandum 33-601, Jet Propulsion Laboratory, March 15, 1973.

APPENDICES

APPENDIX 1

Link and Arm Transformations

Individual Link Transformations

$$T_0^1 = \begin{bmatrix} c_1 & 0 & -s_1 & 0 \\ s_1 & 0 & c_1 & 0 \\ 0 & -1 & 0 & r_1 \\ 0 & 0 & 0 & 1 \end{bmatrix} \qquad T_1^2 = \begin{bmatrix} c_2 & 0 & s_2 & 0 \\ s_2 & 0 & -c_2 & 0 \\ 0 & 1 & 0 & r_2 \\ 0 & 0 & 0 & 1 \end{bmatrix}$$

$$T_2^3 = \begin{bmatrix} 0 & 1 & 0 & 0 \\ -1 & 0 & 0 & 0 \\ 0 & 0 & 1 & r_3 \\ 0 & 0 & 0 & 1 \end{bmatrix} \qquad T_3^4 = \begin{bmatrix} c_4 & 0 & -s_4 & 0 \\ s_4 & 0 & c_4 & 0 \\ 0 & -1 & 0 & 0 \\ 0 & 0 & 0 & 1 \end{bmatrix}$$

$$T_4^5 = \begin{bmatrix} c_5 & 0 & s_5 & 0 \\ s_5 & 0 & -c_5 & 0 \\ 0 & 1 & 0 & 0 \\ 0 & 0 & 0 & 1 \end{bmatrix} \qquad T_5^6 = \begin{bmatrix} c_6 & -s_6 & 0 & 0 \\ s_6 & c_6 & 0 & 0 \\ 0 & 0 & 1 & r_6 \\ 0 & 0 & 0 & 1 \end{bmatrix}$$

Arm Transformation

$$T = T_0^6 = \begin{bmatrix} \vec{n} & \vec{s} & \vec{a} & \vec{p} \\ 0 & 0 & 0 & 1 \end{bmatrix}$$

$$\vec{n} = \begin{bmatrix} c_{1256}\, s_4 + s_1\, c_{456} - c_{16}\, s_{25} + c_{124}\, s_6 - s_{146} \\ s_{14}\, c_{256} - c_{1456} - s_{125}\, c_6 + s_{16}\, c_{24} + c_1\, s_{46} \\ -s_{24}\, c_{56} - c_{26}\, s_5 - s_{26}\, c_4 \end{bmatrix}$$

$$\vec{s} = \begin{bmatrix} -c_{125}\, s_{46} - s_{16}\, c_{45} + c_1\, s_{256} + c_{1246} - s_{14}\, c_6 \\ -s_{146}\, c_{25} + c_{145}\, s_6 + s_{1256} + s_1\, c_{246} + c_{16}\, s_4 \\ s_{246}\, c_5 + c_2\, s_{56} - s_2\, c_{46} \end{bmatrix}$$

$$\vec{a} = \begin{bmatrix} c_{12}\, s_{45} + s_{15}\, c_4 + c_{15}\, s_2 \\ s_{145}\, c_2 - c_{14}\, s_5 + s_{12}\, c_5 \\ c_{25} - s_{245} \end{bmatrix}$$

$$\vec{p} = \begin{bmatrix} r_3\, c_1\, s_2 - r_2\, s_1 \\ r_3\, s_1\, s_2 + r_2\, c_1 \\ r_3\, c_2 + r_1 \end{bmatrix} + r_6 \vec{a}$$

NOTE: $s_i \equiv \sin\theta_i \quad c_i \equiv \cos\theta_i$

$s_{ij} \equiv \sin\theta_i \sin\theta_j$

$c_{ijk} = \cos\theta_i \cos\theta_j \cos\theta_k$, etc.

APPENDIX 2

Kinematic Solutions

2a) Direct Solution

Define the vector

$$\vec{d} = \begin{bmatrix} d_1 \\ d_2 \\ d_3 \end{bmatrix} = \vec{p} - r_6 \vec{a} - \begin{bmatrix} 0 \\ 0 \\ r_1 \end{bmatrix} .$$

Observing that

$$\vec{d} = \begin{bmatrix} r_3 c_1 s_2 - r_2 s_1 \\ r_3 s_1 s_2 + r_2 c_1 \\ r_3 c_2 \end{bmatrix} ,$$

it is seen that

$$r_3 = \sqrt{d^2 - r_2^2} \tag{1}$$

and that there is no solution if Eq. (1) does not yield an $r_3 \in [14.0, 111.8]$.

The cosine of θ_2 is then uniquely determined by

$$c_2 = \frac{d_3}{r_3} \tag{2}$$

Thus there are two possible values of θ_2, one each corresponding to

$$s_2 = \pm \frac{\sqrt{d_1^2 + d_2^2 - r_2^2}}{r_3} ,$$

yielding one left arm value for θ_2 (positive) and one right arm value (negative). If $|\theta_2| > 175$ deg, there is no physically achievable solution.

Solving the system

$$(r_3\ s_2)\ c_1 - (r_2)\ s_1 = d_1$$

$$(r_2)\ c_1 + (r_3\ s_2)\ s_1 = d_2$$

yields the solution for θ_1 given by

$$\theta_1 = \tan^{-1}\left[\left(\frac{d_2\ r_3\ s_2 - d_1\ r_2}{d_1\ r_3\ s_2 + d_2\ r_2}\right)\right] . \qquad (3)$$

Knowing θ_1, θ_2 and r_3 permits calculation of the base system - boom transformation T_0^3 given by

$$T_0^3 = \begin{bmatrix} s_1 & c_1c_2 & c_1s_2 & r_3c_1s_2 - r_2s_1 \\ -c_1 & s_1c_2 & s_1s_2 & r_3s_1s_2 + r_2c_1 \\ 0 & -s_2 & c_2 & r_3c_2 + r_1 \\ 0 & 0 & 0 & 1 \end{bmatrix} .$$

Considering T_0^3 as being of the form

$$\begin{bmatrix} \vec{x}_3 & \vec{y}_3 & \vec{z}_3 & \vec{p}_3 \\ 0 & 0 & 0 & 1 \end{bmatrix}$$

and defining

$$\vec{z} = \frac{\vec{z}_3 \times \vec{a}}{\|\vec{z}_3 \times \vec{a}\|} = \begin{bmatrix} -s_1 s_4 + c_1 c_2 c_4 \\ c_1 s_4 + s_1 c_2 c_4 \\ -s_2 c_4 \end{bmatrix} ,$$

the following are true:

$$s_4 = \vec{y}_3 \times \vec{z} \cdot \vec{z}_3 \qquad c_4 = \vec{y}_3 \cdot \vec{z}$$

$$s_5 = \vec{z}_3 \times \vec{a} \cdot \vec{z} \qquad c_5 = \vec{z}_3 \cdot \vec{a}$$

$$s_6 = \vec{z} \times \vec{s} \cdot \vec{a} \qquad c_6 = \vec{z} \cdot \vec{s}$$

Thus

$$\theta_4 = \tan^{-1}\left[\frac{\vec{y}_3 \times \vec{z} \cdot \vec{z}_3}{\vec{y}_3 \cdot \vec{z}}\right] , \tag{4}$$

$$\theta_5 = \tan^{-1}\left[\frac{\vec{z}_3 \times \vec{a} \cdot \vec{z}}{\vec{z}_3 \cdot \vec{a}}\right] , \tag{5}$$

$$\theta_6 = \tan^{-1}\left[\frac{\vec{z} \times \vec{s} \cdot \vec{a}}{\vec{z} \cdot \vec{s}}\right] . \tag{6}$$

Given θ_2, these values yield one solution.
$\vec{\theta} = (\theta_1, \theta_2, r_3, \theta_4, \theta_5, \theta_6)$ satisfies $T(\vec{\theta}) = T$, then so does

$$\hat{\vec{\theta}} = (\theta_1, \theta_2, r_3, \theta_4 + \pi, -\theta_5, \theta_6 + \pi) \quad , \tag{7}$$

giving two solutions for each of the two possible values of θ_2.

2b) Incremental Solution

Given a joint variable vector $\bar{\vec{\theta}}$, the arm transformation $\bar{T} \equiv T(\bar{\vec{\theta}})$ is defined. The problem is to find the vector $\vec{\theta}$, where

$$\vec{\theta} \equiv \bar{\vec{\theta}} + \delta\vec{\theta} \quad ,$$

yielding an arm transformation T differing from $\bar{T}$ by a small amount

$$\Delta T \equiv T - \bar{T} \quad .$$

For convenience, several simplifying definitions are introduced:

$$A_i \equiv T^i_{i-1}(\theta_i)$$

$$\bar{A}_i \equiv T^i_{i-1}(\bar{\theta}_i) \quad ,$$

$$Q_i \equiv \left\{ \begin{bmatrix} 0 & -1 & 0 & 0 \\ 1 & 0 & 0 & 0 \\ 0 & 0 & 0 & 0 \\ 0 & 0 & 0 & 0 \end{bmatrix} \text{for } i \neq 3 \text{ and } \begin{bmatrix} 0 & 0 & 0 & 0 \\ 0 & 0 & 0 & 0 \\ 0 & 0 & 0 & 1 \\ 0 & 0 & 0 & 0 \end{bmatrix} \text{for } i = 3 \right\}$$

and

$$\bar{U}_i \equiv \bar{A}_1 \ldots \bar{A}_{i-1} Q_i \bar{A}_i \ldots \bar{A}_6 \quad ,$$

all for $i = 1 \ldots 6$.

Using the approximations

$$\sin(\bar{\theta}_i + \delta\theta_i) \approx \sin\bar{\theta}_i + \cos\bar{\theta}_i\,\delta\theta_i \quad ,$$

$$\cos(\bar{\theta}_i + \delta\theta_i) \approx \cos\bar{\theta}_i - \sin\bar{\theta}_i\,\delta\theta_i \quad ,$$

and $$\delta\theta_i\,\delta\theta_j \approx 0 \quad ,$$

it is seen that

$$A_i \equiv T^i_{i-1}(\theta_i) \equiv T^i_{i-1}(\bar{\theta}_i + \delta\theta_i) \approx A(\bar{\theta}_i) + Q_i A_i(\bar{\theta}_i)\,\delta\theta_i$$

$$= \bar{A}_i + Q_i \bar{A}_i\,\delta\theta_i$$

or

$$A_i \approx (I + Q_i\,\delta\theta_i)\,\bar{A}_i \tag{1}$$

By definition of T,

$$A_1 A_2 \cdots A_6 = T \quad ,$$

Substituting from Eq. (1),

$$\bar{A}_1 \cdots \bar{A}_6 + Q_1 \bar{A}_1 \cdots \bar{A}_6\,\delta\theta_1 + \bar{A}_1 Q_2 \bar{A}_2 \cdots \bar{A}_6\,\delta\theta_2 + \cdots + \bar{A}_1 \cdots \bar{A}_5 Q_6 \bar{A}_6 = T \quad ,$$

or

$$\bar{U}_1\,\delta\theta_1 + \cdots + \bar{U}_6\,\delta\theta_6 = T - \bar{T} = \Delta T \tag{2}$$

This matrix relation contains 16 equations in six unknowns; all quantities except the $\delta\theta_i$ are known. Thus, six independent elements must be selected.

Suppose we wish to consider the original hand system rotated first about its normal axis by α and then "tilted" about the sliding axis by ϵ. The new hand orientation vectors can then be transformed by the original arm transformation T back to the base system and changes in position of $(\Delta x, \Delta y, \Delta z)$ added. That is,

$$T = \Delta P \overline{T} R \quad , \tag{3}$$

where

$$\Delta P = \begin{bmatrix} 1 & 0 & 0 & \Delta x \\ 0 & 1 & 0 & \Delta y \\ 0 & 0 & 1 & \Delta z \\ 0 & 0 & 0 & 1 \end{bmatrix}$$

and

$$R = \begin{bmatrix} c_\epsilon & 0 & s_\epsilon & 0 \\ 0 & 1 & 0 & 0 \\ -s_\epsilon & 0 & c_\epsilon & 0 \\ 0 & 0 & 0 & 1 \end{bmatrix} \begin{bmatrix} 1 & 0 & 0 & 0 \\ 0 & c_\alpha & s_\alpha & 0 \\ 0 & -s_\alpha & c_\alpha & 0 \\ 0 & 0 & 0 & 1 \end{bmatrix} \approx \begin{bmatrix} 1 & 0 & \epsilon & 0 \\ 0 & 1 & \alpha & 0 \\ -\epsilon & -\alpha & 1 & 0 \\ 0 & 0 & 0 & 1 \end{bmatrix} .$$

Observe that the small rotations α and ϵ are with respect to the hand system; had it been desired to implement rotations with respect to the base system, we would have $T = \Delta P R \overline{T}$. Changes in position are with respect to the base system.

Considering $\overline{T}$ as of the form

$$\begin{bmatrix} \overline{n}_1 & \overline{s}_1 & \overline{a}_1 & \overline{x} \\ \overline{n}_2 & \overline{s}_2 & \overline{a}_2 & \overline{y} \\ \overline{n}_3 & \overline{s}_3 & \overline{a}_3 & \overline{z} \\ 0 & 0 & 0 & 1 \end{bmatrix} ,$$

the rotated and translated arm transformation T becomes, on substitution into Eq. (2),

$$T = \begin{bmatrix} -\epsilon\bar{a}_1 & -\alpha\bar{a}_1 & \alpha\bar{s}_1 + \epsilon\bar{n}_1 & \Delta x \\ -\epsilon\bar{a}_2 & -\alpha\bar{a}_2 & \alpha\bar{s}_2 + \epsilon\bar{n}_2 & \Delta y \\ -\epsilon\bar{a}_3 & -\alpha\bar{a}_3 & \alpha\bar{s}_3 + \epsilon\bar{n}_3 & \Delta z \\ 0 & 0 & 0 & 0 \end{bmatrix} + \overline{T} \tag{4}$$

The expanded matrix in Eq. (4), then, is ΔT.

Selecting for the six required independent equations those corresponding to the first three elements in the last $(\Delta\vec{P})$ column of ΔT, two from the third column $(\Delta\vec{a})$, and one from the second column $(\Delta\vec{s})$, Eq. (2) might look like

$$\begin{bmatrix} \overline{U}_1(1,4) & \overline{U}_2(1,4) & \cdots & \overline{U}_6(1,4) \\ \overline{U}_1(2,4) & \overline{U}_2(2,4) & \cdots & \overline{U}_6(2,4) \\ \overline{U}_1(3,4) & \overline{U}_2(3,4) & \cdots & \overline{U}_6(3,4) \\ \overline{U}_1(3,3) & \overline{U}_2(3,3) & \cdots & \overline{U}_6(3,3) \\ \overline{U}_1(2,3) & \overline{U}_2(2,3) & \cdots & \overline{U}_6(2,3) \\ U_1(3,2) & \overline{U}_2(3,2) & \cdots & \overline{U}_6(3,2) \end{bmatrix} \begin{bmatrix} \delta\theta_1 \\ \delta\theta_2 \\ \delta r_3 \\ \delta\theta_4 \\ \delta\theta_5 \\ \delta\theta_6 \end{bmatrix} = \begin{bmatrix} \Delta T_{14} \\ \Delta T_{24} \\ \Delta T_{34} \\ \Delta T_{33} \\ \Delta T_{23} \\ \Delta T_{32} \end{bmatrix} = \begin{bmatrix} \Delta x \\ \Delta y \\ \Delta z \\ \alpha\bar{s}_3 + \epsilon\bar{n}_3 \\ \alpha\bar{s}_2 + \epsilon\bar{n}_2 \\ -\alpha\bar{a}_3 \end{bmatrix} \tag{5}$$

Therefore, as an example, to find the change $\delta\vec{\theta}$ in the joint variable vector $\vec{\theta}$ required to implement a small change in position $(\Delta x, \Delta y, \Delta z)$ with no change in orientation, Eq. (5) would be applied with $\alpha = \epsilon = 0$.

APPENDIX 3

Trajectory Specifications

Define a normalized time

$$u = \frac{\tau - \tau_{i-1}}{\tau_i - \tau_{i-1}} , \quad \tau \in [\tau_{i-1}, \tau_i]$$

running from 0 at the beginning of a trajectory segment i (when time $\tau = \tau_{i-1}$) to 1 at the end ($\tau = \tau_i$) for i = 1 ... n. The trajectory is the sequence of polynomials $h_i(u)$ which together form $\theta(\tau)$. If $t_i \equiv \tau_i - \tau_{i-1}$ is the time required for the i^{th} trajectory segment, then the following hold:

$$\text{position} \qquad h_i(u) = \theta(\tau) = h\left(\frac{\tau - \tau_{i-1}}{t_i}\right) ,$$

$$\text{velocity} \qquad v_i(u) = \dot{\theta}(\tau) = h_i'(u)/t_i ,$$

and

$$\text{acceleration} \qquad a_i(u) = \ddot{\theta}(\tau) = h_i''(u)/t_i^2$$

Therefore

$$h_i(0) = \theta_{i-1} \quad \text{and} \quad h_i(1) = \theta_i, \; i = 1, \ldots, n ,$$

and we define

$$\text{velocities} \qquad v_i \equiv v_i(1) = h_i'(1)/t_i ,$$

$$\text{the initial velocity} \qquad v_0 \equiv v_1(0) ,$$

$$\text{the accelerations} \qquad a_i \equiv a_i(1) = h_i''(1)/t_i^2 ,$$

$$\text{and the initial acceleration} \qquad a_0 \equiv a_1(0) .$$

As shown in Fig. 1, then,

$$h_i(u): \; (\theta_{i-1}, v_{i-1}, a_{i-1}) \rightarrow (\theta_i, v_i, a_i) .$$

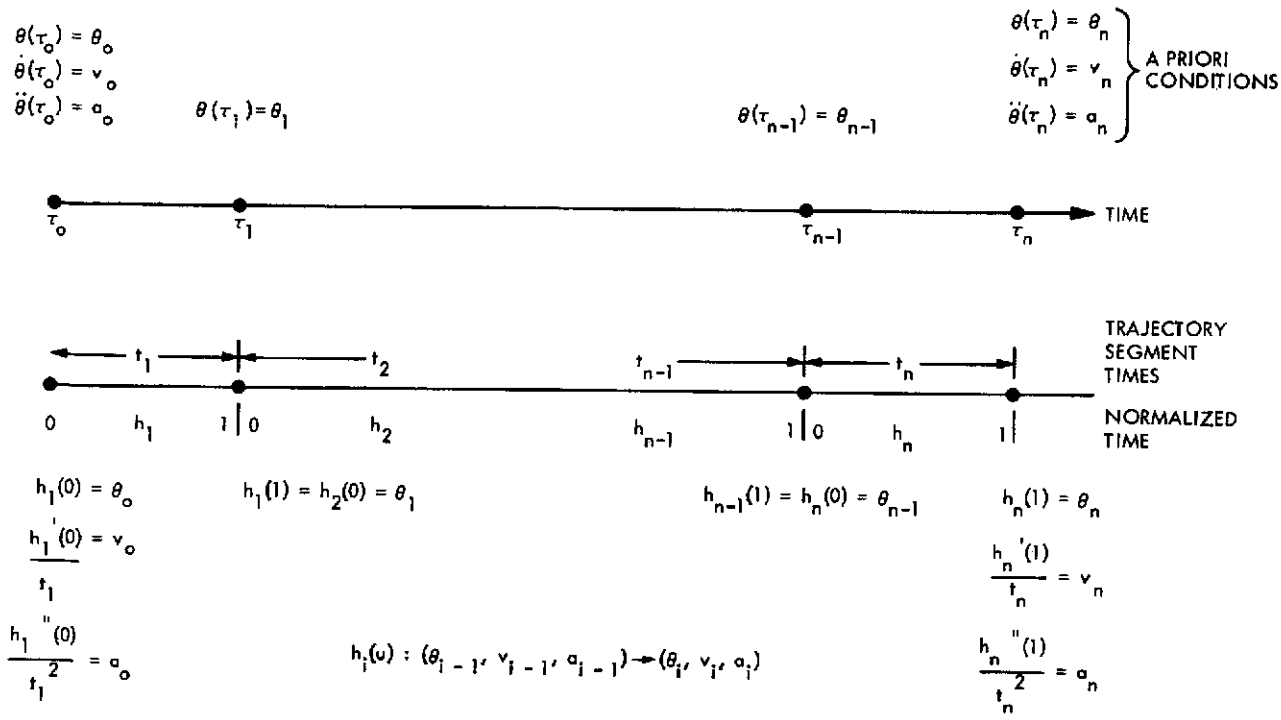

Fig. 1. Trajectory Parameters

Table 1 specifies the 14 constraints for (4, 3, 4) and (3, 5, 3) trajectories, and Tables 2 through 4 detail the trajectory polynomials for these two trajectories and one consisting of five cubics.

Table 1. Conditions for the (4, 3, 4) and (3, 5, 3) trajectories

1	$h_1(0) = \theta_0$	Initial conditions
2	$h_1'(0) = v_0 t_1$	
3	$h_1''(0) = a_0 t_1^2$	
4	$h_3(1) = \theta_3$	Terminal conditions
5	$h_3'(1) = v_3 t_3$	
6	$h_3''(1) = a_3 t_3^2$	
7	$h_1(1) = \theta_1$	Intermediate conditions
8	$h_2(1) = \theta_2$	
9	$h_2(0) = h_1(1)$	Continuous position
10	$h_3(0) = h_2(1)$	
11	$\frac{h_2'(0)}{t_2} = \frac{h_2'(1)}{t_1}$	Continuous velocity
12	$\frac{h_3'(0)}{t_3} = \frac{h_2'(1)}{t_2}$	
13	$\frac{h_2''(0)}{t_2^2} = \frac{h_1''(1)}{t_1^2}$	Continuous acceleration
14	$\frac{h_3''(0)}{t_3^2} = \frac{h_2''(1)}{t_2^2}$	

Table 2. The (4, 3, 4) trajectory

$$h_1(u) = (\theta_0) + (v_0 t_1)\,u + \left(\frac{a_0 t_1^2}{2}\right)u^2 + (x)\,u^3 + \left(\delta_1 - v_0 t_1 - \frac{a_0 t_1^2}{2} - x\right)u^4$$

$$(\theta_0, v_0, a_0) \rightarrow (\theta_1, v_1, a_1)$$

$$v_1 = \frac{4\delta_1}{t_1} - 3v_0 - a_0 t_1 - \frac{x}{t_1}$$

$$a_1 = \frac{12\delta_1}{t_1^2} - \frac{12v_0}{t_1} - 5a_0 - \frac{6x}{t_1^2}$$

$$\delta_i \equiv \theta_i - \theta_{i-1}$$

$$h_2(u) = (\theta_1) + (v_1 t_2)\,u + \left(\frac{a_1 t_2^2}{2}\right)u^2 + \left(\delta_2 - v_1 t_2 - \frac{a_1 t_2^2}{2}\right)u^3$$

$$(\theta_1, v_1, a_1) \rightarrow (\theta_2, v_2, a_2)$$

$$v_2 = \frac{3\delta_2}{t_2} - 2v_1 - \frac{a_1 t_2}{2}$$

$$a_2 = \frac{6\delta_2}{t_2^2} - \frac{6v_1}{t_2} - 2a_1 t_2$$

$$h_3(u) = (\theta_2) + (v_2 t_3)\,u + \left(\frac{a_2 t_3^2}{2}\right)u^2 + \left(-8\delta_3 + 5v_3 t_3 - \frac{a_3 t_3^2}{2} + 3v_2 t_3\right)u^3$$

$$+ \left(9\delta_3 - 4v_2 t_3 - \frac{a_2 t_3^2}{2} - 5v_3 t_3 + \frac{a_3 t_3^2}{2}\right)u^4$$

$$(\theta_2, v_2, a_2) \rightarrow (\theta_3, v_3, a_3)$$

where

$$x = \frac{\left[2\delta_1\left(4 + \frac{2t_3}{t_2} + \frac{2t_3}{t_1} + \frac{3t_2}{t_1}\right) - \frac{\delta_2 t_1}{t_2}\left(3 + \frac{t_3}{t_2}\right) + \frac{2\delta_3 t_1}{t_3} - v_0 t_1\left(6 + \frac{6t_2}{t_1} + \frac{4t_3}{t_1} + \frac{3t_3}{t_2}\right) - v_3 t_1 - a_0 t_1 t_3\left(\frac{5}{3} + \frac{t_1}{t_2} + \frac{2t_1}{t_3} + \frac{5t_2}{2t_3}\right) + \frac{a_3 t_1 t_3}{6}\right]}{\left[\frac{t_3}{t_2} + \frac{2t_3}{t_1} + 2 + \frac{3t_2}{t_1}\right]}$$

Table 3. The (3,5,3) trajectory

$$h_1(u) = (\theta_0) + (v_0\, t_1)\, u + \left(\frac{a_0\, t_1^2}{2}\right) u^2 + \left(\delta_1 - v_0\, t_1 - \frac{a_0\, t_1^2}{2}\right) u^3$$

$$(\theta_0,\ v_0,\ a_0) \rightarrow (\theta_1,\ v_1,\ a_1)$$

$$v_1 = \frac{3\delta_1}{t_1} - 2v_0 - \frac{a_0\, t_1}{2}$$

$$a_1 = \frac{6\delta_1}{t_1^2} - \frac{6v_0}{t_1} - 2a_0$$

$$h_3(u) = (\theta_2) + \left(3\delta_3 - 2v_3\, t_3 + \frac{a_3\, t_3^2}{2}\right) u + (-3\delta_3 + 3v_3\, t_3 - a_3\, t_3^2)\, u^2$$

$$+ \left(\delta_3 - v_3\, t_3 + \frac{a_3\, t_3^2}{2}\right) u^3$$

$$(\theta_2,\ v_2,\ a_2) \rightarrow (\theta_3,\ v_3,\ a_3)$$

$$v_2 = \frac{3\delta_3}{t_3} - 2v_3 + \frac{a_3\, t_3}{2}$$

$$a_2 = \frac{-6\delta_3}{t_3^2} + \frac{6v_3}{t_3} - 2a_3$$

$$h_2(u) = (\theta_1) + (v_1\, t_2)\, u + \left(\frac{a_1\, t_2^2}{2}\right) u^2 + \left(10\delta_2 - 6v_1\, t_2 - 4v_2\, t_2 - \frac{3a_1\, t_2^2}{2} + \frac{a_2\, t_2^2}{2}\right) u^3$$

$$+ \left(-15\delta_2 + 8v_1\, t_2 + 7v_2\, t_2 + \frac{3a_1\, t_2^2}{2} - a_2\, t_2^2\right) u^4$$

$$+ \left(6\delta_2 - 3v_1\, t_2 - 3v_2\, t_2 + \frac{a_2\, t_2^2}{2} - \frac{a_1\, t_2^2}{2}\right) u^5$$

$$(\theta_1,\ v_1,\ a_1) \rightarrow (\theta_2,\ v_2,\ a_2)$$

Table 4. Five Cubics

$$h_1(u) = (\theta_0) + (v_0 t_1) u + \left(\frac{a_0 t_1^2}{2}\right) u^2 + \left(\delta_1 - v_0 t_1 - \frac{a_0 t_1^2}{2}\right) u^3$$

$$(\theta_0, v_0, a_0) \rightarrow (\theta_1, v_1, a_1) \qquad v_1 = \frac{3\delta_1}{t_1} - 2v_0 - \frac{a_0 t_1}{2} \qquad a_1 = \frac{6\delta_1}{t_1^2} - \frac{6v_0}{t_1} - 2a_0$$

$$h_5(u) = (\theta_4) + \left(3\delta_5 - 2v_5 t_5 + \frac{a_5 t_5^2}{2}\right) u + (-3\delta_5 + 3v_5 t_5 - a_5 t_5^2) u^2 + \left(\delta_5 - v_5 t_5 + \frac{a_5 t_5^2}{2}\right) u^3$$

$$(\theta_4, v_4, a_4) \rightarrow (\theta_5, v_5, a_5) \qquad v_4 = \frac{3\delta_5}{t_5} - 2v_5 + \frac{a_5 t_5}{2} \qquad a_4 = \frac{-6\delta_5}{t_5^2} + \frac{6v_5}{t_5} - 2a_5$$

$$h_2(u) = (\theta_1) + (v_1 t_2) u + \left(\frac{a_1 t_2^2}{2}\right) u^2 + (x_1) u^3$$

$$(\theta_1, v_1, a_1) \rightarrow (\theta_2, v_2, a_2) \qquad \theta_2 = \theta_1 + v_1 t_2 + \frac{a_1 t_2^2}{2} + x_1$$

$$v_2 = v_1 + a_1 t_2 + \frac{3x_1}{t_2} \qquad a_2 = a_1 + \frac{6x_1}{t_2^2}$$

$$h_3(u) = (\theta_2) + (v_2 t_3) u + \left(\frac{a_2 t_3^2}{2}\right) u^2 + (x_2) u^3$$

$$(\theta_2, v_2, a_2) \rightarrow (\theta_3, v_3, a_3) \qquad \theta_3 = \theta_2 + v_2 t_3 + \frac{a_2 t_3^2}{2} + x_2$$

$$v_3 = v_2 + a_2 t_3 + \frac{3x_2}{t_3} \qquad a_3 = a_2 + \frac{6x_2}{t_3^2}$$

$$h_4(u) = (\theta_3) + (v_3 t_4) u + \left(\frac{a_3 t_4^2}{2}\right) u^2 + (x_3) u^3$$

$$(\theta_3, v_3, a_3) \rightarrow (\theta_4, v_4, a_4)$$

where

$$x_1 = t_2^2 D_1/D \qquad x_2 = t_3^2 D_2/D \qquad x_3 = t_4^2 D_3/D$$

$$D_1 = k_1 (t - t_2) + k_2 (t_4^2 - d) - k_3 [(t - t_4) d + t_4^2 (t_4 - t_2)]$$

$$D_2 = -k_1 (t + t_3) + k_2 (c - t_4^2) + k_3 [(t - t_4) c + t_4^2 (t - t_2)]$$

$$D_3 = k_1 (t - t_4) + k_2 (d - c) + k_3 [(t_4 - t_2) c - d (t - t_2)]$$

$$D = t (t - t_2) (t - t_4) \qquad t = t_2 + t_3 + t_4$$

$$k_1 = \Delta\theta - v_1 t - a_1 t^2/2 \qquad k_2 = (\Delta v - a_1 t - \Delta a t/2)/3$$

$$k_3 = \Delta a/6 \qquad c = 3t^2 - 3t t_2 + t_2^2$$

$$d = 3t_4^2 + 3t_3 t_4 + t_3^2 \qquad \Delta\theta = \theta_4 - \theta_1$$

$$\Delta v = v_4 - v_1 \qquad \Delta a = a_4 - a_1$$

APPENDIX 4

Relations Used in Obstacle Detection

The minimum distance d_0 between two lines

$$\vec{P} \equiv \vec{P}_0 + \alpha\,(\vec{P}_1 - \vec{P}_0)$$

and

$$\vec{Q} \equiv \vec{Q}_0 + \beta\,(\vec{Q}_1 - \vec{Q}_0) \quad ,$$

where

$$\alpha,\ \beta \in [0,\ 1]$$

and $\vec{v} \equiv \vec{P}_1 - \vec{P}_0 \qquad \vec{w} \equiv \vec{Q}_0 - \vec{Q}_1 \qquad \vec{u} \equiv \vec{P}_0 - \vec{Q}_0$

is given by

$$d_0 = \left\| u + \alpha_0 \vec{v} + \beta_0 \vec{w} \right\| \quad ,$$

where

$$\alpha_0 = \langle 0,\ \hat{\alpha},\ 1 \rangle \quad , \quad \beta_0 = \langle 0,\ \hat{\beta},\ 1 \rangle \quad ,$$

the relation $\langle a,\ b,\ c \rangle \equiv \begin{cases} b \text{ if } b \in [a,\ c] \\ a \text{ if } b < a \\ c \text{ if } b > c \end{cases}$

and $\hat{\alpha} = \begin{cases} \dfrac{(\vec{u} \cdot \vec{w})\,(\vec{v} \cdot \vec{w}) - (\vec{u} \cdot \vec{v})\,(\vec{w} \cdot \vec{w})}{\vec{v}^2\,\vec{w}^2 - (\vec{v} \cdot \vec{w})^2} & \text{if } \|\vec{v} \cdot \vec{w}\| \neq \|\vec{v}\|\,\|\vec{w}\| \\ -(\vec{u} \cdot \vec{v})/(\vec{v} \cdot \vec{v}) & \text{otherwise} \end{cases}$

$\hat{\beta} = \begin{cases} \dfrac{(\vec{v} \cdot \vec{w})\,(\vec{u} \cdot \vec{v}) - (\vec{v} \cdot \vec{v})\,(\vec{u} \cdot \vec{w})}{\vec{v}^2\,\vec{w}^2 - (\vec{v} \cdot \vec{w})^2} & \text{if } \|\vec{v} \cdot \vec{w}\| \neq \|\vec{v}\|\,\|\vec{w}\| \\ 0 & \text{otherwise} \end{cases}$

The minimum distance between a point $\vec{Q}_0 = \vec{Q}_1$ and a line $\vec{P}$ is given by the same relations. Since $\vec{Q}_0 = \vec{Q}_1$, then $\vec{w} = 0$ and $\|\vec{v} \cdot \vec{w}\| = \|\vec{v}\|\,\|\vec{w}\| = 0$. Thus $\hat{\alpha} = -(u \cdot v)/(v \cdot v)$ and $\hat{\beta} = 0$.

Link equations

line $\quad \vec{P} \quad \vec{P}_0 + \alpha(\vec{P}_1 - \vec{P}_0) \quad , \quad \alpha \in [0, 1]$

	$\vec{P}_0$	$\vec{P}_1$
link 1 (post)	$\begin{bmatrix} 0 \\ 0 \\ 0 \end{bmatrix}$	$\begin{bmatrix} 0 \\ 0 \\ r_1 \end{bmatrix}$
link 2 (shoulder)	$\begin{bmatrix} 30.48 s_1 \\ -30.48 c_1 \\ r_1 \end{bmatrix}$	$\begin{bmatrix} -r_2 s_1 \\ r_2 c_1 \\ r_1 \end{bmatrix}$
link 3 (boom)	$\begin{bmatrix} -r_2 s_1 + (r_3 - 111.8) c_1 s_2 \\ r_2 c_1 + (r_3 - 111.8) s_1 s_2 \\ r_1 + (r_3 - 111.8) c_2 \end{bmatrix}$	$\begin{bmatrix} r_3 c_1 s_2 - r_2 s_1 \\ r_3 s_1 s_2 + r_2 c_1 \\ r_3 c_2 + r_1 \end{bmatrix}$
link 6 (hand)	$\begin{bmatrix} r_3 c_1 s_2 - r_2 s_1 \\ r_3 s_1 s_2 + r_2 c_1 \\ r_3 c_2 + r_1 \end{bmatrix}$	$\vec{P}_0 + r_6 \vec{a}$

$$\vec{a} = \begin{bmatrix} c_{12} s_{45} + s_{15} c_4 + c_{15} s_2 \\ s_{145} c_2 - c_{14} s_5 + s_{12} c_5 \\ c_{25} - s_{245} \end{bmatrix}$$

APPENDIX 5

Equations of Motion

5a) General Derivation

T^i_j, i, j = 0, . . . , 6, is the transformation relating coordinate systems i and j, and the velocity V_i in the base reference frame of a point

$$R_i = \begin{bmatrix} x_i \\ y_i \\ z_i \\ 1 \end{bmatrix}$$

on link i is given by

$$V_i = \frac{d}{dt}\left(T^i_0 R_i\right) \tag{1}$$

or, alternatively, as

$$V_i = \left(\sum_j \frac{\partial T^i_0}{\partial q_j}\,\dot{q}_j\right) R_i \ , \tag{2}$$

where q_i are the components of the joint-variable vector.

Note that V_i is expressed in system 0, the base frame, and R_i in system i.

Defining

$$Q_i = \begin{bmatrix} 0 & -1 & 0 & 0 \\ 1 & 0 & 0 & 0 \\ 0 & 0 & 0 & 0 \\ 0 & 0 & 0 & 0 \end{bmatrix}$$

for i = 1, 2, 4, 5, 6 and

$$Q_3 = \begin{bmatrix} 0 & 0 & 0 & 0 \\ 0 & 0 & 0 & 0 \\ 0 & 0 & 0 & 1 \\ 0 & 0 & 0 & 0 \end{bmatrix} ,$$

then

$$\frac{\partial T_{i-1}^{i}}{\partial q_i} = Q_i \, T_{i-1}^{i} \tag{3}$$

and

$$\frac{\partial T_0^i}{\partial q_j} = \begin{cases} T_0^1 \, T_1^2 \cdots T_{j-2}^{j-1} \, Q_j \, T_{j-1}^{j} \cdots T_{i-1}^{i} & \text{for } j \le i \\ 0 & \text{for } j > i \end{cases} \tag{4}$$

Defining the partial derivative in Eq. (4) as U_{ij} and combining products, we have

$$U_{ij} \equiv \frac{\partial T_0^i}{\partial q_j} = \left\{ \begin{array}{ll} T_0^{j-1} \, Q_j \, T_{j-1}^{i} & i \ge j \\ 0 & i < j \end{array} \right\} . \tag{5}$$

We will also have occasion to refer to the derivative

$$\frac{\partial U_{ij}}{\partial q_k} \quad ,$$

referred to as U_{ijk} and given by

$$U_{ijk} \equiv \frac{\partial U_{ij}}{\partial q_k} = \begin{cases} T_0^{j-1} Q_j T_{j-1}^{k-1} Q_k T_{k-1}^{i} & i \geq k \geq j \\ T_0^{k-1} Q_k T_{k-1}^{j-1} Q_j T_{j-1}^{i} & i \geq j \geq k \\ 0 & i < j \text{ or } i < k \end{cases} \tag{6}$$

Observe that $U_{ijk} = U_{ikj}$.

The expression of velocity in Eq. (2) then becomes

$$V_i = \left(\sum_{j=1}^{6} U_{ij} \dot{q}_j \right) R_i = \left(\sum_{j=1}^{i} U_{ij} \dot{q}_j \right) R_i \; . \tag{7}$$

We now turn our attention to the total kinetic energy of (the six links of) the arm. The kinetic energy K of the system and K_i of link i, i = 1, ..., 6, are expressed in the base reference system. For link i,

$$dK_i = \frac{1}{2} \left(\dot{x}_i^2 + \dot{y}_i^2 + \dot{z}_i^2 \right) d_m = \frac{1}{2} \mathrm{Tr} \left(V_i V_i^T \right) d_m \; .$$

Using Eq. (7), it is seen that

$$dK_i = \frac{1}{2} \mathrm{Tr} \left[\sum_{p=1}^{i} U_{ip} \dot{q}_p R_i \sum_{r=1}^{i} (U_{ir} \dot{q}_r R_i)^T \right] d_m$$

$$= \frac{1}{2} \mathrm{Tr} \left[\sum_{p=1}^{i} \sum_{r=1}^{i} U_{ip} R_i R_i^T U_{ir}^T \dot{q}_p \dot{q}_r \right] d_m$$

$$= \frac{1}{2} \mathrm{Tr} \left[\sum_{p=1}^{i} \sum_{r=1}^{i} U_{ip} \left(R_i d_m R_i^T \right) U_{ir}^T \dot{q}_p \dot{q}_r \right] . \qquad (8)$$

The matrix U_{ij} is the rate of change of the points on link i relative to the base frame as q_j changes; it is constant for all points on the link and independent of the mass distribution of the link. The $\dot{q}_j$'s are also independent of mass distribution, so

$$K_i = \int dK_i = \frac{1}{2} \mathrm{Tr} \left[\sum_{p=1}^{i} \sum_{r=1}^{i} U_{ip} \left(\int R_i R_i^T d_m \right) U_{ir}^T \dot{q}_p \dot{q}_r \right] \qquad (9)$$

Defining as J_i (i = 1, . . . , 6) and expanding the integral in Eq. (9) yields

$$J_i \equiv \int R_i R_i^T d_m = \begin{bmatrix} \int x_i^2 d_m & \int x_i y_i d_m & \int x_i z_i d_m & \int x_i d_m \\ \int x_i y_i d_m & \int y_i^2 d_m & \int y_i z_i d_m & \int y_i d_m \\ \int x_i z_i d_m & \int y_i z_i d_m & \int z_i^2 d_m & \int z_i d_m \\ \int x_i d_m & \int y_i d_m & \int z_i d_m & \int d_m \end{bmatrix} .$$

Recalling that the inertia tensor I_{ij} can be expressed as

$$I_{ij} = \begin{cases} I^*_{ij} & \text{if } i = j \\ -I^*_{ij} & \text{if } i \neq j \end{cases}$$

where

$$I^*_{ij} = \int \left[\delta_{ij} \left(\sum_k x_k^2 \right) - x_i x_j \right] d_m ,$$

then J_i can be expressed as

$$J_i = \begin{bmatrix} \frac{-I_{xx} + I_{yy} + I_{zz}}{2} & I_{xy} & I_{xz} & m_i \bar{x}_i \\ I_{xy} & \frac{I_{xx} - I_{yy} + I_{zz}}{2} & I_{yz} & m_i \bar{y}_i \\ I_{xz} & I_{yz} & \frac{I_{xx} + I_{yy} - I_{zz}}{2} & m_i \bar{z}_i \\ m_i \bar{x}_i & m_i \bar{y}_i & m_i \bar{z}_i & m_i \end{bmatrix} , \quad (10)$$

and the kinetic energy of the arm as

$$K = \sum_{i=1}^{6} K_i = \frac{1}{2} \sum_{i=1}^{6} \mathrm{Tr} \left[\sum_{p=1}^{i} \sum_{r=1}^{i} U_{ip} J_i U_{ir}^T \dot{q}_p \dot{q}_r \right] . \quad (11)$$

Since matrix sum and trace operations commute and the scalar multiplications can be equivalently performed on the trace,

$$K = \frac{1}{2} \sum_{i=1}^{6} \sum_{j=1}^{i} \sum_{k=1}^{i} \left[\mathrm{Tr} \left(U_{ij} J_i U_{ik}^T \right) \dot{q}_j \dot{q}_k \right] . \tag{12}$$

Observe that the J_i are dependent only upon the mass distribution of the links and not their position or rate of motion. Thus the J_i need only be computed once.

The potential energies P_i of links i in the base frame sum to the total potential energy

$$P = \sum_{i=1}^{6} P_i = \sum_{i=1}^{6} - m_i G \left(T_0^i \bar{R}_i \right) , \tag{13}$$

where G is the gravity vector expressed in the base frame. For a level vehicle, $G = (0, 0, -|g|, 0)$.

Forming the Lagrangian $L \equiv K - P$ and then applying the Euler Lagrange equation

$$F_i = \frac{d}{dt} \frac{\partial L}{\partial \dot{q}_i} - \frac{\partial L}{\partial q_i}, \quad i = 1, \ldots, 6, \tag{14}$$

for the generalized force (torque for all joints but the third) results in the equations of motion

$$F_i = \sum_{j=i}^{6} \sum_{k=1}^{j} \mathrm{Tr} \left(U_{jk} J_j U_{ji}^T \right) \ddot{q}_k + \sum_{j=i}^{6} \sum_{k=1}^{j} \sum_{m=1}^{j} \mathrm{Tr} \left(U_{jkm} J_j U_{ji}^T \right) \dot{q}_k \dot{q}_m$$

$$- \sum_{j=i}^{6} m_j G U_{ji} \bar{R}_j , \qquad i = 1, \ldots, 6. \tag{15}$$

This relation is derived in Appendix 5b.

These equations can be simplified somewhat by introducing three new definitions:

$$D_{ij} \equiv - m_j GU_{ji} \bar{R}_j ,$$

$$D_{ijk} \equiv Tr\left(U_{jk} J_j U_{ji}^T\right) ,$$

and

$$D_{ijkm} \equiv Tr\left(U_{jkm} J_j U_{ji}^T\right).$$

It follows from the definitions of the U's that $D_{ij} = 0$ for $i > j$, $D_{ijk} = 0$ for $k > j$ or $i > j$, and $D_{ijkm} = 0$ for $k > j$, $m > j$, or $i > j$.

The equations of motion (15) can be expressed as

$$F_i = \sum_{j=i}^{6} \sum_{k=1}^{j} D_{ijk} \ddot{q}_k + \sum_{j=i}^{6} \sum_{k=1}^{j} \sum_{m=1}^{j} D_{ijkm} \dot{q}_k \dot{q}_m + \sum_{j=i}^{6} D_{ij}$$

or, rearranging summations, as

$$F_i = \sum_{k=1}^{6} \sum_{j=i}^{6} D_{ijk} \ddot{q}_k + \sum_{k=1}^{6} \sum_{m=1}^{6} \sum_{j=i}^{6} D_{ijkm} \dot{q}_k \dot{q}_m + \sum_{j=i}^{6} D_{ij} . \qquad (16)$$

Extra terms added by the rearrangement are all zero. The rearrangement permits separation of purely dynamic factors from link position and mass distribution-dependent terms when Eq. (16) is written as

$$F_i = \sum_{k=1}^{6} C_{ik} \ddot{q}_k + \sum_{k=1}^{6} \sum_{m=1}^{6} C_{ikm} \dot{q}_k \dot{q}_m + C_i , \qquad (17)$$

where

$$C_{ik} \equiv \sum_{j=\max(i,k)}^{6} D_{ijk} = \sum_{j=\max(i,k)}^{6} \mathrm{Tr}\left(U_{jk} J_j U_{ji}^T\right)$$

$$C_{ikm} \equiv \sum_{j=\max(i,k,m)}^{6} D_{ijkm} = \sum_{j=\max(i,k,m)}^{6} \mathrm{Tr}\left(U_{jkm} J_j U_{ji}^T\right) \quad ,$$

and

$$C_i \equiv \sum_{j=i}^{6} D_{ij} = \sum_{j=i}^{6} (-m_j \, GU_{ji} \, \bar{R}_j).$$

5b) Derivation of Equation (15)*

The Lagrangian $L = K - P$ is, from Eqs. (12) and (13),

$$L = \frac{1}{2} \sum_{i=1}^{6} \sum_{j=1}^{i} \sum_{k=1}^{i} \mathrm{Tr}\left(U_{ij} J_i U_{ik}^T\right) \dot{q}_j \dot{q}_k + \sum_{i=1}^{6} m_i G T_0^i \bar{R}_i \, .$$

Before proceeding, we observe the following the facts:

$$\text{(A1)} \quad \frac{\partial}{\partial \dot{q}_p} \mathrm{Tr}\left(U_{ij} J_i U_{ik}^T\right) = \mathrm{Tr}\left[\frac{\partial}{\partial \dot{q}_p}\left(U_{ij} J_i U_{ik}^T\right)\right] = 0 \, ,$$

since the U's are dependent only on the joint variable and not its rate of change, and since J_i is also independent of the rate of change of any joint variable.

$$\text{(A2)} \quad \frac{\partial T_0^i}{\partial \dot{q}_p} = 0 .$$

$$\text{(A3)} \quad \frac{\partial T_0^i}{\partial q_p} = U_{ip} \text{ (from Eq. 5).}$$

$$\text{(A4)} \quad D_{kij} \equiv \mathrm{Tr}\left(U_{ij} J_i U_{ik}^T\right) = \mathrm{Tr}\left[\left(U_{ij} J_i U_{ik}^T\right)^T\right] = \mathrm{Tr}\left(U_{ik} J_i U_{ij}^T\right) \equiv D_{jik}$$

(J_i is symmetric).

$$\text{(A5)} \quad \frac{dU_{ij}}{dt} = \sum_{m=1}^{6} \frac{\partial U_{ij}}{\partial q_m} \dot{q}_m = \sum_{m=1}^{6} U_{ijm} \dot{q}_m = \sum_{m=1}^{i} U_{ijm} \dot{q}_m$$

(from Eq. (6)).

*Equation numbers refer to Appendix 5a.

$$\frac{d}{dt} D_{kij} = \frac{d}{dt} Tr\left(U_{ij} J_i U_{ik}^T\right) = Tr\left(\frac{dU_{ij}}{dt} J_i U_{ik}^T\right)$$

$$+ Tr\left(U_{ij} \frac{dJ_i}{dt} U_{ik}^T\right) + Tr\left(\frac{dU_{ik}}{dt} J_i U_{ij}^T\right)$$

$$= Tr\left(\sum_{m=1}^{i} U_{ijm} J_i U_{ik}^T \dot{q}_m\right) + 0 + Tr\left(\sum_{m=1}^{i} U_{ikm} J_i U_{ij}^T \dot{q}_m\right)$$

$$= \sum_{m=1}^{i} Tr\left(U_{ijm} J_i U_{ik}^T\right) \dot{q}_m + \sum_{m=1}^{i} Tr\left(U_{ikm} J_i U_{ij}^T\right) \dot{q}_m . \tag{A6}$$

$$\frac{\partial L}{\partial \dot{q}_p} = \frac{1}{2} \sum_{i=1}^{6} \sum_{j=1}^{i} \sum_{k=1}^{i} D_{kij} \left(\dot{q}_k \delta_{jp} + \dot{q}_j \delta_{kp}\right) + 0$$

$$= \frac{1}{2} \sum_{i=1}^{6} \sum_{k=1}^{6} D_{kip} \dot{q}_k + \frac{1}{2} \sum_{i=1}^{6} \sum_{j=1}^{i} D_{pij} \dot{q}_j$$

$$= \sum_{i=1}^{6} \sum_{k=1}^{i} D_{pik} \dot{q}_k = \sum_{i=p}^{6} \sum_{k=1}^{i} Tr\left(U_{ik} J_i U_{ip}^T\right) \dot{q}_k \tag{A7}$$

$$\frac{d}{dt} \frac{\partial L}{\partial \dot{q}_p} = \sum_{i=p}^{6} \sum_{k=1}^{i} \ddot{q}_k D_{pik} + \sum_{i=p}^{6} \sum_{k=1}^{i} \sum_{m=1}^{i} Tr\left(U_{ikm} J_i U_{ip}^T\right) \dot{q}_k \dot{q}_m$$

$$+ \sum_{i=p}^{6} \sum_{k=1}^{i} \sum_{m=1}^{i} Tr\left(U_{ipm} J_i U_{ik}^T\right) \dot{q}_k \dot{q}_m \tag{A8}$$

(A9) $$\frac{\partial}{\partial q_p} D_{kij} = \frac{\partial}{\partial q_p} \operatorname{Tr}\left(U_{ij} J_i U_{ik}^T\right) = \operatorname{Tr}\left(U_{ijp} J_i U_{ik}^T\right) + \operatorname{Tr}\left(U_{ikp} J_i U_{ij}^T\right)$$

$$\frac{\partial L}{\partial q_p} = \frac{1}{2} \sum_{i=1}^{6} \sum_{j=1}^{i} \sum_{k=1}^{i} \frac{\partial}{\partial q_p} (D_{kij})\, \dot{q}_j \dot{q}_k + \sum_{i=1}^{6} m_i G \frac{\partial T_0^i}{\partial q_p} \bar{R}_i$$

$$= \frac{1}{2} \sum_{i=p}^{6} \sum_{j=1}^{i} \sum_{k=1}^{i} \operatorname{Tr}\left(U_{ijp} J_i U_{ik}^T\right) \dot{q}_j \dot{q}_k$$

(A10) $$+ \frac{1}{2} \sum_{i=p}^{6} \sum_{j=1}^{i} \sum_{k=1}^{i} \operatorname{Tr}\left(U_{ikp} J_i U_{ij}^T\right) \dot{q}_j \dot{q}_k + \sum_{i=1}^{6} m_i G U_{ip} \bar{R}_i .$$

With these observations in hand, the Euler Lagrange equations

$$F_p = \frac{d}{dt} \frac{\partial L}{\partial \dot{q}_p} - \frac{\partial L}{\partial q_p}$$

become

$$F_p = \sum_{i=p}^{6} \sum_{k=1}^{i} D_{pik} \ddot{q}_k + \sum_{i=p}^{6} \sum_{k=1}^{i} \sum_{m=1}^{i} \operatorname{Tr}\left(U_{ikm} J_i U_{ip}^T\right) \dot{q}_k \dot{q}_m$$

$$+ \sum_{i=p}^{6} \sum_{k=1}^{i} \sum_{m=1}^{i} \operatorname{Tr}\left(U_{ipm} J_i U_{ik}^T\right) \dot{q}_k \dot{q}_m$$

$$- \frac{1}{2} \sum_{i=p}^{6} \sum_{j=1}^{i} \sum_{k=1}^{i} \operatorname{Tr}\left(U_{ijp} J_i U_{ik}^T\right) \dot{q}_j \dot{q}_k$$

$$-\frac{1}{2}\sum_{i=p}^{6}\sum_{j=1}^{i}\sum_{k=1}^{i}\mathrm{Tr}\left(U_{ikp}J_iU_{ij}^T\right)\dot{q}_j\dot{q}_k-\sum_{i=p}^{6}m_iGU_{ip}\bar{R}_i\,.$$

Since $U_{ijk} = U_{ikj}$ and dummy indices of summation abound above, we can reindex and then note that the third, fourth, and fifth terms above cancel. Changing dummy indices, we have

$$F_i=\sum_{j=i}^{6}\sum_{k=1}^{j}\mathrm{Tr}\left(U_{jk}J_jU_{ji}^T\right)\ddot{q}_k$$

$$+\sum_{j=i}^{6}\sum_{k=1}^{j}\sum_{m=1}^{j}\mathrm{Tr}\left(U_{jkm}J_jU_{ji}^T\right)\dot{q}_k\dot{q}_m-\sum_{j=i}^{6}m_jGU_{ji}\bar{R}_j\,,$$

as advertised.

APPENDIX 6

Proofs of Coefficient Propositions

Proposition 1: $C_{ik} = C_{ki}$

Pf:

$$C_{ik} = \sum_{j=\max\{i,k\}}^{6} \mathrm{Tr}\left(U_{jk} J_j U_{ji}^T\right).$$

Since $\mathrm{Tr}(A) = \mathrm{Tr}(A^T)$ and $J_j^T = J_j$,

$$C_{ik} = \sum_{j=\max\{i,k\}}^{6} \mathrm{Tr}\left(U_{ji} J_j U_{jk}^T\right) \equiv C_{ki}.$$

Thus the coefficient for the reaction force on link i due to the acceleration of link k is equal to the reaction force coefficient for link k due to the acceleration of link i. This statement is in some sense analogous to a restatement of Newton's third law. Thus C_{ik} is symmetric and contains only 21 unique elements.

Proposition 2: $C_{ikm} = C_{imk}$

Pf:

$$C_{ikm} = \sum_{j=\max\{i,k,m\}}^{6} \mathrm{Tr}\left(U_{jkm}\, J_j\, U_{ji}^T\right).$$

Since $U_{jkm} = U_{jmk}$, the statement is proven. Clearly the effect on link i of the velocities of links k and m is the same as that of the velocities of links m and k. Of the 216 C_{ikm}, only 126 are unique.

Proposition 3: $C_{i3m} = 0,\ m \geq 3.$

Pf:

$$C_{i3m} = \sum_{j=\max\{m,i\}}^{6} \mathrm{Tr}\left(T_0^2\, Q_3\, T_2^{m-1}\, Q_m\, T_{m-1}^{j}\, J_j\, T_{i-1}^{jT}\, Q_i^T\, T_0^{i-1T}\right)$$

Now

$$Q_3 T_2^{m-1} = Q_3 = \begin{bmatrix} 0 & 0 & 0 & 0 \\ 0 & 0 & 0 & 0 \\ 0 & 0 & 0 & 1 \\ 0 & 0 & 0 & 0 \end{bmatrix},$$

since row 4 of $T_2^{m-1} = (0,\ 0,\ 0,\ 1)$.

Furthermore, since $Q_3 Q_m = 0$ for all m, then so does $Q_3 T_2^{m-1} Q_m$, and so also does the whole matrix in parentheses above. Thus the trace and hence C_{i3m} $(m \geq 3) = 0$. Thus it is seen that the boom (link 3) velocity and the three wrist link velocities do not have any interactive effect on any of the six joints. Of the 126 unique C_{ikm}, 24 are zero and thus only 102 need ever be calculated.

Proposition 4: $C_{ikm} = -C_{mki}$ for $i,\ m \geq k$

(Corollary 1: $C_{iki} = 0,\ i \geq k$

Corollary 2: $C_{kkk} = 0$)

Pf: Assume without loss of generality that $m \geq i$. Then

$$C_{ikm} = \sum_{j=m}^{6} Tr\left(T_0^{k-1} Q_k T_{k-1}^{m-1} Q_m T_{m-1}^{j} J_j T_{i-1}^{j\ T} Q_i^T T_0^{i-1T}\right)$$

$$= \sum_{j=m}^{6} Tr\left(T_0^{k-1} Q_k T_{k-1}^{m-1} Q_m T_{m-1}^{j} J_j T_{i-1}^{j\ T} Q_i^T T_{k-1}^{i-1T} T_0^{k-1T}\right) .$$

Since $Tr(X) = Tr(X^T)$,

$$C_{ikm} = \sum_{j=m}^{6} T_r\left(T_0^{k-1} T_{k-1}^{i-1} Q_i T_{i-1}^{j} J_j T_{m-1}^{jT} Q_m^T T_{k-1}^{m-1T} Q_k^T T_0^{k-1T}\right) .$$

Let

$$A \equiv T_0^{k-1} ,$$

a link transformation matrix, and

$$B \equiv T_{k-1}^{i-1} Q_i\ T_{i-1}^{j} J_j T_{m-1}^{jT} Q_m^T T_{k-1}^{m-1T} .$$

Then

$$C_{ikm} = \sum_{j=m}^{6} Tr\left(ABQ_k^T A^T\right).$$

Since

$$C_{mki} = \sum_{j=m}^{6} \mathrm{Tr}\left(T_0^{k-1} Q_k T_{k-1}^{i-1} Q_i T_{i-i}^{j} J_j T_{m-1}^{jT} Q_m^T T_0^{m-1T}\right)$$

$$= \sum_{j=m}^{6} \mathrm{Tr}\left(AQ_k BA^T\right) ,$$

it need only be shown that

$$\mathrm{Tr}\left(AQ_k BA^T\right) = -\mathrm{Tr}\left(ABQ_k^T A^T\right) ,$$

where A and B are defined above. In proposition 3, it was shown that $C_{i3m} = 0$ for $m \geq 3$ and for arbitrary i. Thus $C_{i3m} = -C_{m3i} = 0$, so we need only prove the above relationship for $k \neq 3$.

As a link transformation matrix, A is of the form

$$A = \begin{bmatrix} n_1 & s_1 & a_1 & p_1 \\ n_2 & s_2 & a_2 & p_2 \\ n_3 & s_3 & a_3 & p_3 \\ 0 & 0 & 0 & 1 \end{bmatrix} ,$$

where $\vec{n}$, $\vec{s}$, and $\vec{a}$ are mutually orthogonal unit vectors. Utilization of this and straightforward multiplication of the matrices above gives us

$$\mathrm{Tr}\left(ABQ_k^T A^T\right) = b_{21} - b_{12} + b_{41}(\vec{s} \cdot \vec{p}) - b_{42}(\vec{n} \cdot \vec{p})$$

and

$$\mathrm{Tr}\left(AQ_k BA^T\right) = -b_{21} + b_{12} + b_{14}(\vec{s} \cdot \vec{p}) - b_{24}(\vec{n} \cdot \vec{p}) .$$

It will be shown that $b_{4j} = b_{j4} = 0$, $j = 1, \ldots, 4$, thus proving that the traces are in fact equal in magnitude but opposite in sign and hence that $C_{ikm} = -C_{mki}$ $(i, m \geq k)$, as claimed.

B is of the form

$$B = TQXQ^T T^T ,$$

where the T's are link transformations. Thus row 4 of T (column 4 of T^T) is (0, 0, 0, 1). Also, row 4 of Q (column 4 of Q^T) is (0, 0, 0, 0). So row 4 of TQ and column 4 of $Q^T T^T$ are therefore all 0, and hence so are the fourth row and column of B. QED.

The link i force coefficient for the coupled velocities of links k and m is equal and opposite to the link m force coefficient of the coupled velocities of links k and i for $k \leq m, i$. Thus outer links' (i and m) velocities act reflexively to each other as they interact with the velocity of an inner link (k). Observe that though the coefficients are equal in magnitude, the force contributions are not, for in one case the force contribution is $C_{ikm}\dot{q}_k\dot{q}_m$ and in the other case the contribution is $- C_{ikm}\dot{q}_k\dot{q}_i$. The coefficient is multiplied by a different factor.

Corollary 1 indicates that there is no interactive effect on any outer link (i) due to coupling of its own velocity with that of any inner link (k). Corollary 2 merely restates that the centrifugal force of a rotary joint is radial in direction and thus creates no torque felt by the motor.

Only 56 of the C_{ikm} need be computed. With the 21 C_{ik} and six C_i, only 83 C's are left. In fact, if the vehicle is gravitationally horizontal (i.e., the gravity vector $\vec{G} = (0, 0, g, 0)$), then there are only five gravity terms C_i to compute..

Proposition 5: $C_1 = 0$ if $\vec{G} = (0, 0, g, 0)$.

Pf:

$$C_1 = \sum_{j=1}^{6} (-m_j GU_{j1}\bar{R}_j) = \sum_{j=1}^{6} \left(-m_j GQ_1 T_0^j \bar{R}_j\right) .$$

Since $\vec{G}Q_1 = \vec{0}$, $C_1 = 0$ also.

APPENDIX 7

Implemented Control Stack Functions

NUMBER	NAME	ACTION
00	TRAJ	execute five cubic trajectory
01	INCREM	execute incremental-quintic trajectory
02	FORCE	exert force or moment
03	RD POTS	read pots
04	OPEN	open hand
05	CLOSE	close hand
06	RD DYN	read dynamics (tachs, error torque, computed torque) after next command
07		
10	WAIT	wait
11		
12		
13		
14		
15		
16		
17	FINI	end-of-group

NASA — JPL — Coml., L.A., Calif.